Bone Microenvironment-Suppressed T Cells Increase Osteoclast Formation and Osteolytic Bone Metastases in Mice

Danna L. Arellano,[1,2] Patricia Juárez,[1,3] Andrea Verdugo-Meza,[1,2] Paloma S. Almeida-Luna,[1,2] Juan A. Corral-Avila,[1,2] Florian Drescher,[1,2] Felipe Olvera,[4] Samanta Jiménez,[1] Bennett D. Elzey,[5,6] Theresa A. Guise,[3,7,8] and Pierrick G.J. Fournier[1,3]

[1]Biomedical Innovation Department, Centro de Investigación Científica y de Educación Superior de Ensenada (CICESE), Ensenada
[2]Posgrado en Ciencias de la Vida, Centro de Investigación Científica y de Educación Superior de Ensenada (CICESE), Ensenada, Mexico
[3]Department of Medicine, Indiana University School of Medicine, Indianapolis, IN
[4]Departamento de Biología Molecular y Bioprocesos, Instituto de Biotecnología Universidad Nacional Autónoma de México, Cuernavaca, Mexico
[5]Department of Comparative Pathobiology, Purdue University, West Lafayette, IN, USA
[6]Purdue University Center for Cancer Research, Purdue University, West Lafayette, IN, USA
[7]Endocrine Neoplasia and Hormone Disorders, The University of Texas MD Anderson Cancer Center, Houston, TX, USA
[8]Cancer Prevention and Research Institute of Texas, Austin, TX, USA

ABSTRACT

Immunotherapies use components of the immune system, such as T cells, to fight cancer cells, and are changing cancer treatment, causing durable responses in some patients. Bone metastases are a debilitating complication in advanced breast and prostate cancer patients. Approved treatments fail to cure bone metastases or increase patient survival and it remains unclear whether immunotherapy could benefit patients. The bone microenvironment combines various immunosuppressive factors, and combined with T cell products could increase bone resorption fueling the vicious cycle of bone metastases. Using syngeneic mouse models, our study revealed that bone metastases from 4T1 breast cancer contain tumor-infiltrating lymphocyte (TILs) and their development is increased in normal mice compared to immunodeficient and T-cell depleted mice. This effect seemed caused by the TILs specifically in bone, because T-cell depletion increased 4T1 orthotopic tumors and did not affect bone metastases from RM-1 prostate cancer cells, which lack TILs. T cells increased osteoclast formation ex vivo and in vivo contributing to bone metastasis vicious cycle. This pro-osteoclastic effect is specific to unactivated T cells, because activated T cells, secreting interferon γ (IFNγ) and interleukin 4 (IL-4), actually suppressed osteoclastogenesis, which could benefit patients. However, non-activated T cells from bone metastases could not be activated in ex vivo cultures. 4T1 bone metastases were associated with an increase of functional polymorphonuclear and monocytic myeloid-derived suppressor cells (MDSCs), potent T-cell suppressors. Although effective in other models, sildenafil and zoledronic acid did not affect MDSCs in bone metastases. Seeking other therapeutic targets, we found that monocytic MDSCs are more potent suppressors than polymorphonuclear MDSCs, expressing programmed cell death receptor-1 ligand (PD-L1)$^{+}$ in bone, which could trigger T-cell suppression because 70% express its receptor, programmed cell death receptor-1 (PD-1). Collectively, our findings identified a new mechanism by which suppressed T cells increase osteoclastogenesis and bone metastases. Our results also provide a rationale for using immunotherapy because T-cell activation would increase their anti-cancer and their anti-osteoclastic properties. © 2022 The Authors. *Journal of Bone and Mineral Research* published by Wiley Periodicals LLC on behalf of American Society for Bone and Mineral Research (ASBMR).

KEY WORDS: BONE METASTASIS; T CELLS; OSTEOCLAST; IMMUNOTHERAPY; IMMUNOSUPRESSION; MDSC

Introduction

Breast, prostate, and lung cancer have some of the highest incidences and prevalences in the world,[1] and when patients reach an advanced stage, they are likely to have metastases in their bones: ~40% of lung cancer patients and >70% for breast or prostate cancer.[2] The occurrence of bone metastases decreases the life expectancy of the patients and their quality of life with the development of skeletal-related events, such as fractures, nerve compression, or severe pain. Unfortunately, the currently approved therapies for bone metastases are only palliative and seem to have no or little effect on the overall survival of the patients.[3,4] Therefore, we need to explore and test new strategies to prevent or treat bone metastases.

Immunotherapies aim to increase or activate immune cells, such as T cells, against cancer cells and are a promising strategy for cancer patients.[5] The presence of tumor-infiltrating lymphocytes (TILs) is a good prognosis marker, because patients with more TILs or CD8+ TILs have better survival in multiple types of cancers, including breast cancer.[6] Further activation of TILs using immunotherapy like inhibitors of the immune checkpoints (ie, programmed cell death receptor-1 ligand [PD-L1], programmed cell death receptor-1 [PD-1], cytotoxic T lymphocyte-associated molecule-4 [CTLA-4]) can lead to remission or increase the survival of cancer patients in the clinic.[7] In patients with triple-negative breast cancer, anti-PD-L1 or anti-PD-1 treatments combined with nanoparticle albumin–bound (Nab)-paclitaxel or eribulin can increase the progression-free and overall survival of patients.[8,9] Although established bone metastases are reported to lower the effectiveness of checkpoint inhibition,[10,11] the effects of immunotherapy on the development of bone metastases remain unclear.

To characterize the role of the immune system in bone metastases, mouse models such as humanized mice and syngeneic models where cancer cells derived from tumors in inbred mice are inoculated in mice of the same strain can be used. However, the available information does not provide a clear picture, and there is no consensus on the effect of T cells in bone metastases. Using B16-FL melanoma cells, a form of cancer that is relatively immunogenic and responds well to immunotherapy, Zhang and colleagues[12] found that CD8+ T cells and treatment with a CTLA-4-neutralizing antibody decreased the development of bone metastases supporting the use of immunotherapy. Bidwell and colleagues[13] showed that the detection of spontaneous bone metastases from orthotopic tumors of 4T1.2 cancer cells occurred later in immunocompetent mice compared to NOD–severe combined immunodeficiency (scid)–gamma (NSG) mice that have a defective adaptive and innate immune system. However, CD8+ T cells alone were not responsible for such an effect. The combined depletion of CD8+ T cells and natural killer (NK) cells was necessary to reverse the protection granted and accelerate the occurrence of bone metastases from 4T1.2 cells.[13] In sharp contrast, Monteiro and colleagues[14] characterized how T cells increased the homing of 4T1 cells from the primary tumor in the mammary fat pad to the bones. This effect is due to the activation of T helper 17 (Th17) cells, a subset of CD4+ helper T cells that secrete receptor activator of nuclear factor κB ligand (RANKL), causing an increase at the systemic level. Consequently, mice had an increase in osteoclastic resorption resulting in bone loss and an increased homing of 4T1 cancer cells to bone. These results are consistent with the pro-osteoclastic effect of Th17 cells in rheumatoid arthritis[15] or of

T cells in ovariectomy-induced bone loss.[16] Bone resorption releases the growth factors embedded in the mineralized bone matrix, including insulin-like growth factor (IGF)-I and IGF-II and transforming growth factor-β (TGF-β) that increase the proliferation of cancer cells and the development of bone metastases.[17,18] Thus, any factor that increases bone resorption can indirectly increase bone metastases, and T cells in the proper condition could have a pro-metastatic effect instead of an anti-cancer effect.

Due to these discrepancies regarding T cells and bone metastases, and considering the potential benefit of immunotherapy for patients with bone metastases, we aimed to further characterize the role of T cells on the formation of osteoclasts and the development of osteolytic bone metastases. In this study, we found that, whereas T cells did not infiltrate B16-F1 melanoma or RM-1 prostate cancer bone metastases, non-activated T cells infiltrated the bone metastases of 4T1 breast cancer cells. These T cells increased the formation of osteoclasts ex vivo and in vivo, supporting the development of bone metastases. In contrast, when activated, splenic T cells became anti-osteoclastic. However, T cells from bone metastases could not be activated, likely because of the bone metastasis microenvironment factors such as the metabolically active and immunosuppressive myeloid-derived suppressor cells (MDSCs), including the monocytic MDSCs that expressed the immune checkpoint PD-L1 and were more immunosuppressive than the polymorphonuclear MDSCs. Therefore, our results support the use of immunotherapy to activate T cells and treat patients with bone metastases.

Materials and Methods

Cell lines

Mouse cell lines 4T1 (mammary cancer; ATCC #CRL-2539), B16-F1 (melanoma; ATCC #CRL-6323), and TRAMP-C1 (prostate cancer; ATCC #CRL-2730) were obtained from the American Type Culture Collection (ATCC), Manassas, VA, USA. The mouse breast cancer cell line PyMT-R221A was kindly donated by Dr. Connor Lynch (Moffit Cancer Center),[19] and prostate cancer cell line RM-1 was obtained from Dr. Timothy Thompson (The University of Texas, MD Anderson Cancer Center).[20]

4T1 and RM-1 were cultured in Roswell Park Memorial Institute (RPMI) media (Corning, Inc., Corning, NY, USA) supplemented with 10% heat-inactivated fetal bovine serum (FBS) (Atlanta Biologicals, Flowery Branch, GA, USA or Biowest USA, Riverside, MO, USA). TRAMP-C1 and B16-F1 were cultured in RPMI media (Corning) supplemented with 5% FBS. PyMT-R221A were cultured in high-glucose Dulbecco's modified Eagle medium (DMEM) media (Corning) supplemented with 10% FBS. All media also were supplemented with 1% of an antibiotic/antimycotic solution (Corning), and cells were maintained at 37°C with 5% CO_2 in a humidified chamber.

Animal studies

Animal protocols were approved by the Institutional Animal Care and Use Committee at Indiana University (approval numbers 3554 and 10675) or performed in accordance with the Federal Regulation for Animal Experimentation and Care (SAGARPA, NOM-062-ZOO, 1999, Mexico) at the Center of Scientific Research and Higher Education of Ensenada (CICESE). At Indiana University, Balb/C and Balb/C SCID mice were obtained from The Jackson Laboratory (Bar Harbor, ME, USA), and

C57BL/6 mice from Envigo (Placentia, CA, USA). At the CICESE, Balb/C mice were obtained from Envigo and C57BL/6 from the animal care facility at the Universidad Autónoma Metropolitana-Unidad Xochimilco (see Table S1 for more information regarding the characteristics of the mice). Mice received water and food (2018 Teklad Global 18% protein rodent diet; Teklad, Madison, WI, USA) ad libitum and were housed with a 12-hour light/night cycle. They were acclimated for at least 1 week before starting the experiments. Animals bearing tumor were carefully monitored for signs of distress and discomfort and were humanely euthanized when these were confirmed.

Bone metastasis models

A single-cell suspension of 4T1 or B16-F1 was prepared and inoculated (1×10^5 cells in 100 μL of phosphate-buffered saline [PBS]) in the left cardiac ventricle of 6-week-old mice anesthetized with ketamine/xylazine using a 26G needle. 4T1 cells were inoculated in female Balb/C or Balb/C SCID mice, and B16-F1 in female C57BL/6 mice. RM-1 cells (1×10^4 cells in 25 μL of PBS) were inoculated in the tibia of anesthetized 6-week-old male C57BL/6 mice, using a 29G needle.[21] Mice inoculated with 4T1 cells can start showing respiration problems and dying 11 days after the inoculation and were, therefore, euthanized at 10 days, using pentobarbital or ketamine/xylazine overdose, followed by cervical dislocation, and bones were collected. Mice inoculated with RM-1 cells were euthanized 21 days after the inoculation. Mice that died during the intracardiac or the intratibial inoculation were not included in the analysis, as well as mice that had no evidence of osteolysis or had to be euthanized for ethical reasons (signs of pain, stress, difficulty to breathe, or paralysis) before the end of the experiment.

Mammary fat pad tumor model

Six-week-old female Balb/C mice were inoculated in the lower mammary fat pad with 4T1 cells (1×10^5 cells in 50 μL of PBS) using a 29G needle. Tumor size was followed by measuring tumor diameters with a caliper twice per week, and tumor volume was calculated using the formula: tumor volume = $(L \times W^2)/2$, where L and W represent length and width, respectively. After euthanasia using pentobarbital overdose, followed by cervical dislocation, tumors were excised. Mice that had to be euthanized for ethical reasons (signs of pain, stress, extended necrosis on the tumors) before reaching the end of the experiment were excluded from the analysis.

In vivo T-cell depletion

To deplete CD4 and CD8 T cells, mice received injections of 100 μg of anti-CD4 and/or anti-CD8 antibodies (Supplemental Table S2). Control mice received 100 μg of isotype immunoglobulin G2 (IgG2) antibody. All injections were made i.p., using a volume of 100 μL, every 7 days. In bone metastasis experiments, after the inoculation of the cancer cells and once mice fully recovered from the ketamine-xylazine anesthesia (4 hours minimum), they were randomly allocated to the different groups and treatment was initiated. In mammary fat pad tumor experiments, 7 days after the inoculation of 4T1 cells, tumor volume was measured and mice distributed into two groups with nonstatistically different tumor volume, and treatment was initiated.

In vivo treatments

Zoledronic acid monohydrate (Sigma-Aldrich, St. Louis, MO, USA) was resuspended in PBS. Mice were inoculated with PBS or zoledronic acid, at a dose of 25 μg/kg (s.c.), three times a week (Supplemental Table S3). Sildenafil citrate (Sigma-Aldrich) was resuspended at a concentration of 100 μg/μL in dimethylsulfoxide (DMSO) and further diluted to 3.4 μg/μL in a solution of PBS–polyethylene glycol (PEG) 400 (5:4 ratio) prior to inoculation in mice at a dose of 20 mg/kg (i.p.), every 2 days. Mice were randomly allocated to the different groups and treatment was initiated 1 day after the intracardiac inoculation of 4T1 cells.

Osteoclastogenesis assay

Bone marrow cells from hindlimbs (tibia and femur) were flushed and erythrocytes were removed using a red blood cell lysis buffer (155mM NH_4Cl, 10mM $NaHCO_3$, 1mM EDTA). In flat-bottom 96-well plates, 40×10^3 bone marrow cells were cultured in α minimum essential medium (α-MEM) supplemented with 10% FBS (Biowest USA), macrophage colony-stimulating factor (M-CSF) (25 ng/mL; PeproTech, Rocky Hill, NJ, USA, or BioLegend, San Diego, CA, USA), and RANKL (12.5–25 ng/mL; PreproTech or BioLegend) (Supplemental Table S3). Half of the media was renewed every 2 days, and cells were monitored for the appearance of large-size cells. After 5 to 8 days of culture, cells were stained for tartrate resistant acid phosphatase (TRAP) activity (Sigma-Aldrich) and the number of osteoclasts (TRAP+ multinucleated cells) was counted using a microscope.

T cells were isolated from the spleen of mice by negative selection using Dynabeads Untouched mouse T cells kits (Invitrogen, Carlsbad, CA, USA) following the manufacturer's recommendations. To isolate T cells from the bone marrow, we used first the Dynabeads Untouched mouse T cells kit followed by the MojoSort mouse CD3 selection kit (BioLegend). The percentage of T cells in the isolated fraction was confirmed by flow cytometry. When appropriate, T cells were activated ex vivo by culturing them in flat-bottom 96-well plates coated with an anti-CD3 antibody in RPMI media supplemented with 5% FBS, 55μM β-mercaptoethanol, 5 μg/mL anti-CD3 and 5 μg/mL anti-CD28 antibodies (Supplemental Table S2). T cells were added to the osteoclastogenesis assay 1 day after seeding the bone marrow cells.

Flow cytometry analysis

Blood, spleen, and bone marrow cells were obtained from mice inoculated or not with cancer cells. Peripheral blood mononuclear cells (PBMCs) were collected from the retro-orbital sinus using heparinized capillaries. Bone marrow cells were prepared flushed from the hindlimbs. Spleen cell suspensions were obtained grinding spleens between two frosted glass slides. Erythrocytes were removed using a red blood cell lysis buffer (155mM NH_4Cl, 10mM $NaHCO_3$, 1mM EDTA), live cells were counted and centrifuged (350g, 5 minutes, 4°C), washed twice with isolation buffer (PBS 1X, 1% bovine serum albumin [BSA], and 0.5mM EDTA), resuspended in a blocking buffer containing True Stain Monocyte Blocker (BioLegend), an anti-CD16/32 antibody, and FBS (10% vol/vol). T cells were then labeled using fluorescently labeled antibodies against mouse CD90.2, CD3ε, CD4, CD8α, CD25, CD62L, CD69, CTLA-4, and PD-1. For intracellular staining, cell suspensions were cultured in the presence of phorbol 12-myristate 13-acetate (50 ng/mL) and ionomycine (750 ng/mL) for 2 hours. Brefeldin A (5 μg/mL) was added to

the media and the cells were further cultured for 3 hours. After blocking the cells and performing the staining of cell surface markers, cells were fixed and permeabilized using CytoFix/CytoPerm solutions (BD Biosciences, San Jose, CA, USA) or the Fixation/Permeabilization concentrate solution (Thermo Fisher Scientific, Waltham, MA, USA) according to manufacturer's instructions. Intracellular staining was performed using fluorescently labeled antibodies against mouse IFNγ, IL-4, IL-17A, and forkhead box P3 (FoxP3). For the analysis of MDSCs, cells were cultured in the presence of CellROX Orange (Invitrogen) or DAF-2 diacetate (Cayman Chemical, Ann Arbor, MI, USA) for 30 minutes, at 37°C before blocking and staining with fluorescently labeled antibodies against mouse CD11b, Ly6C, Ly6G, and PD-L1. Antibodies were purchased from eBioscience (Santa Clara, CA, USA) or BioLegend; see Supplemental Table S2 for more information. Cells were washed and resuspended in isolation buffer and analyzed immediately after, using an Attune acoustic focusing flow cytometer (Applied Biosystems, Foster City, CA, USA). Single-color compensation samples were prepared using cells or compensation beads (Invitrogen). Samples were analyzed using the Attune software (v2.1; Applied Biosystems). Singlets were gated using foward scatter-area (FSC-A) versus -height (FSC-H), and side scatter-area (SSC-A) versus -height (SSC-H) density plots, and cells were gated using FSC-A versus SSC-A density plots before analyzing the different cell populations. The complete gating strategies can be found in Supplemental Fig. S1. Similarly, single-cell suspensions of cancer cells were stained using a antibody against H-2 (MHC-I). Flow cytometry data were analyzed using either the Attune software (v2.1) or FlowJo (v10.6, BD Bioscience).

MDSC and T cell isolation using cell sorting

Cell suspensions of spleen or bone marrow cells were prepared and erythrocytes were removed using a red blood cell lysis buffer. For myeloid cell studies, $CD11b^+$ cells were enriched using the Magnetic Activated Cell sorting (MACS; Miltenyi Biotec, Bergisch Gladbach, Germany) before staining with fluorescently labeled antibodies against Ly6C and Ly6G and performing a fluorescence-activated cell sorting (FACS) analysis using a iCyt Reflection (Sony, Tokyo, Japan). For T cell studies, cells were stained using an antibody against mouse CD3 before FACS analysis.

T-cell suppression assay

Polymorphonuclear MDSCs (PMN-MDSCs) and monocytic MDSCs (M-MDSCs) were isolated from the pooled bone marrow of mice bearing 4T1 bone metastases and 1×10^5 cells/well were co-cultured with varying ratios of $CD8^+$ T cells in 96-well flat-bottom plates coated or not coated with anti-CD3 (5 μg/mL) and anti-CD28 (2.5 μg/mL) antibodies during 72 hours. $CD8^+$ T cell proliferation was assessed by determining 5-ethynyl-2′-deoxyuridine (EdU) incorporation, the EdU (10μM; Thermo Fisher Scientific) was added to the culture 2 hours prior to the cell preparation. Cells were harvested and stained with an antibody against CD8, and the cells were fixed and EdU-stained using the Click-iT EdU cell proliferation kit (Thermo Fisher Scientific) before flow cytometry analysis.

Dual-energy X-ray absorptiometry and micro-computed tomography

Two days before inoculation of 4T1 breast cancer cells, Balb/C and Balb/C SCID mice were anesthetized using isoflurane, and their bones were analyzed using dual-energy X-ray absorptiometry (DXA) and micro-computed tomography (μCT). Whole-body bone mineral density (BMD) was measured using a PIXImus mouse densitometer (GE Lunar Corp, Madison, WI, USA). Quality control was performed before analysis using a phantom mouse and, for the analysis, mice were placed in a ventral position on a Lunar Piximus tray. All measurements were performed by one person (PGJF). Cancellous bone was analyzed using μCT at the proximal metaphysis of the tibia using a high-resolution imaging system (μCT40; SCANCO Medical AG, Brüttisellen, Switzerland) as described.[22] Trabecular bone outcomes included trabecular bone volume fraction (BV/TV; %), trabecular thickness (Tb.Th; μm), trabecular number (Tb.N; mm^{-1}), trabecular separation (Tb.Sp; μm), and connectivity density (Conn.Dens; mm^{-3}).

Radiography

X-ray imaging of bones was performed after euthanasia using whole mice with a Kubtec Xpert80 digital X-ray imager (Kubtec Medical Imaging, Stratford, CT, USA) or on excised bones using an In-Vivo Xtreme imaging system (Bruker, Kontich, Belgium) at the Laboratorio Nacional de Microscopia Avanzada (Instituto de Biotecnología, UNAM, Cuernavaca, México). The quantification of the area of osteolysis was performed in a blind manner. Each radiograph received a random number using random.org before measuring the area of the radiolucent lesions using ImageJ software (NIH, Bethesda, MD, USA; https://imagej.nih.gov/ij/).[23]

Bone histology and histomorphometry

After mice were euthanized, bones were excised, fixed in 10% buffered formalin for 48 hours, decalcified in 10% EDTA for 2 weeks, and embedded in paraffin wax for sectioning. Longitudinal, mid-sagittal sections 7 μm in thickness from the tibia and femur were cut using a microtome Microm HM 355S (Thermo Fisher Scientific). Tissue sections were stained with hematoxylin and eosin (H&E) or for TRAP activity and prepared for histomorphometric analysis. Section images were collected using a Q-Imaging CCD camera mounted on a Leica DM2500 microscope (Leica Microsystems, Inc., Buffalo Grove, IL, USA) equipped with an automated stage (Applied Scientific Instrumentation, Eugene, OR, USA) or an Axiocam 505 color (Carl Zeiss Microscopy, Inc., Dublin, CA, USA) on an Axio Scope A1 microscope (Carl Zeiss Microscopy). Histomorphometric analysis was also done in a blinded manner and tissue sections received a random number before performing the analysis using either Bioquant Osteo software v12.0 (Bioquant Image Analysis Corporation, Nashville, TN, USA) or ImageJ. Skeletal tumor burden was defined as the area of bone occupied by cancer cells in the tibia and femur, on H&E-stained slides as described.[24] The total bone area defined as the area of both cortical and trabecular bone was calculated at the same sites. Osteoclast number at the tumor-bone interface (Oc.N/BS) in the femur and tibia was measured on TRAP-stained slides.

Immunohistochemistry

Immunohistochemical analysis of tumor-infiltrating lymphocytes was performed on decalcified paraffin-embedded tissue sections using a polyclonal rabbit anti-human/mouse CD3 antibody (DAKO, Carpinteria, CA, USA, or Sigma-Aldrich) (Supplemental Table S2). The staining was performed using

pepsin antigen-retrieval (Sigma-Aldrich), an Avidin/biotin blocking kit (Vector Laboratories, Burlingame, CA, USA), and the VECTASTAIN® Elite ABC kit (Vector Laboratories). Slides were stained using a 3,3, diaminobenzidine substrate kit (Vector Laboratories) and counterstained with hematoxylin.

RNA isolation and quantitative real-time PCR

Single-cell suspensions of spleen and bone marrow of mice inoculated or not inoculated with 4T1 in the left cardiac ventricle were stained with a PE-Cy7 conjugated anti-CD3 antibody (clone 145-2C11; BioLegend) and sorted at the Flow Cytometry Research Facility, a core service of the Indiana University School of Medicine Simon Comprehensive Cancer Center. Using the GenElute Mammalian Total RNA Kit (Sigma-Aldrich), according to the manufacturer's protocol, total RNA was extracted from spleen or bone marrow CD3$^+$ T cells. RNA was extracted immediately after sorting or after activating or not activating T cells using anti-CD3 and anti-CD28 antibodies for 4 days. RNA was reverse-transcribed using anchored oligo dT primers (Thermo Fisher Scientific) and Superscript II reverse transcriptase (Thermo Fisher Scientific). Complementary DNA (cDNA) was analyzed in triplicate by quantitative real-time PCR using HotStart-IT SYBR Green PCR master kit (USB Affymetrix) for 40 cycles (95°C for 15 seconds; 58°C for 30 seconds; 72°C for 30 seconds) on a CFX96 real-time PCR detection system (Bio-Rad Laboratories, Hercules, CA, USA). Primers were designed using Primer3Plus[25] and purchased from Sigma-Aldrich. Quantification of interferon-γ (*Ifng*), interleukin-4 (*Il4*), tumor necrosis factor-α (*Tnfa*), and receptor activator for NF-κB ligand (*Rankl*) gene expression was performed using standard curves of diluted cDNA templates, and relative amounts were normalized to the housekeeping gene β-2 microglobulin (β2m). Primer sequences used were as follows: *Ifng* (sense, 5′-ACTGGCAAAAGGATGGTGAC-3′; antisense 5′-TGAGCTCATTGAATGCTTGG-3′), *Il4* (sense 5′-TCAACCCCCAGC-TAGTTGTC-3′; antisense 5′-TGTTCTTCGTTGCTGTGAGG-3′), *Tnfa* (sense 5′-AGCCCCCAGTCTGTATCCTT-3′; antisense 5′-CTCCC TTTGCAGAACTCAGG-3′), *Rankl* (sense 5′-TGTGTGTTGCTCCCA-CATTT-3′; antisense 5′-TCCCATGGAGCTGGAGTTAC-3′), and *β2m* (sense, 5′-CTGACCGGCCTGTATGCTAT-3′; antisense 5′-CAGTCT-CAGTGGGGGTGAAT-3′).

Statistical and power analyses

For mouse experiments, the smallest number of mice necessary per group was calculated using either Statemate or online platforms (statulator.com and biomath.info) assuming probability of type I and II error rates of α = 0.05 and β = 0.20, respectively. The standard error of the different parameters measured was derived from previous experiments. Statistical analyses were performed using Prism v8 or higher (GraphPad Software, Inc., La Jolla, CA, USA). Tests for normal (Gaussian) distribution were performed using the Shapiro-Wilk test. Comparisons of two groups were conducted using a two-tailed Student's *t* test or Mann-Whitney test. Comparisons of three or more groups were conducted with a one-way analysis of variance (ANOVA) test, followed by a Tukey's or Dunnett's post-test. For responses that were affected by two variables, a two-way ANOVA with a Bonferroni's or Dunnett's post-test was used. Results are presented as box plot with median, interquartile range, and all data points and a $p \leq 0.05$ was considered significantly different.

Results

T cells infiltrate bone metastases of MHC-I$^+$ 4T1 breast cancer cells in mice

To characterize the effect of T cells in bone metastases, we selected first a syngeneic model, screening different mouse cancer cell lines. Using flow cytometry, we assessed the expression of the class I major histocompatibility complex (MHC-I) molecule indispensable for the activation and function of cytotoxic T cells, in TRAMP-C1 and RM-1 prostate cancer cells, 4T1 and PyMT-R221A breast cancer cells, and B16-F1 melanoma cells when compared to PBMCs. We detected very low expression of MHC-I on B16-F1, TRAMP-C1, and RM-1 cells (Fig. 1*A*). In contrast, levels of expression of MHC-I in 4T1 and PyMT-R221A breast cancer cell lines were similar to the levels in PBMCs (Fig. 1*A*).

We inoculated the MHC-I^{lo} RM-1 or B16-F1 melanoma cells or MHC-I^{hi} 4T1 breast cancer cells in the tibia or in the left cardiac ventricle of C57BL/6 or Balb/C mice, respectively, to cause bone metastases. Radiographs indicated that RM-1 and 4T1 cells caused osteolytic lesions whereas the bones of mice inoculated with B16-F1 cells appeared intact (Fig. 1*B*). Histological analysis confirmed the presence of cancer cells in the bone marrow of the mice inoculated with B16-F1, RM-1, or 4T1. TRAP staining indicated the presence of osteoclasts in bone metastases from RM-1 and 4T1 cells, whereas we could not detect osteoclasts in B16-F1 bone metastases, explaining the absence of osteolysis (Fig. 1*B*). To compare the infiltration of T cells, we did immunostaining using an anti-CD3 antibody. Tumor-infiltrating lymphocytes (TILs) were not present in bone metastases from B16-F1 or RM-1 cells, which is consistent with the low expression of MHC-I, whereas we detected TILs in bone metastases caused by 4T1 cells that have a higher expression of MHC-I (Fig. 1*B*). The specificity of the staining was confirmed by the absence of stained cells in 4T1 bone metastasis in Balb/C SCID mice that lack T and B cells (Supplemental Fig. S2*A*). Based on these results, we decided to use both RM-1 prostate and 4T1 breast cancer cells to determine the effect of T cells in bone metastases.

T cells increase osteolytic bone metastases from 4T1 breast cancer cells

To determine whether T cells have an effect on bone metastases, we compared the development of 4T1 bone metastases between Balb/C mice with a functional immune system, and immunodeficient Balb/C SCID mice that lack T and B cells. We first used a DXA scan and μCT to compare the bones of Balb/C and Balb/C SCID mice. The lack of lymphocytes in Balb/C SCID mice did not affect the whole-body BMD or any of the other 3D parameters of the cancellous bone measured (BV/TV, trabecular number, thickness or separation, connectivity density), confirming that the absence of T cells does not cause change in the skeleton of healthy mice (Supplemental Fig. S2*B*). These mice were then inoculated with 4T1 breast cancer cells and the development of bone metastases was assessed 10 days later. Radiographic analysis of the hindlimbs indicated a 3.62-fold increase of the osteolysis area in Balb/C mice compared to Balb/C SCID (Fig. 2*A*). Histomorphometric analysis confirmed that immunocompetent Balb/C mice had a significantly increased skeletal tumor burden (×2.09) and decreased bone area (×0.72) compared to immunodeficient Balb/C SCID mice (Fig. 2*B*). Considering the importance of osteoclasts in the development of bone metastases and the effect of T cells on osteoclast formation in
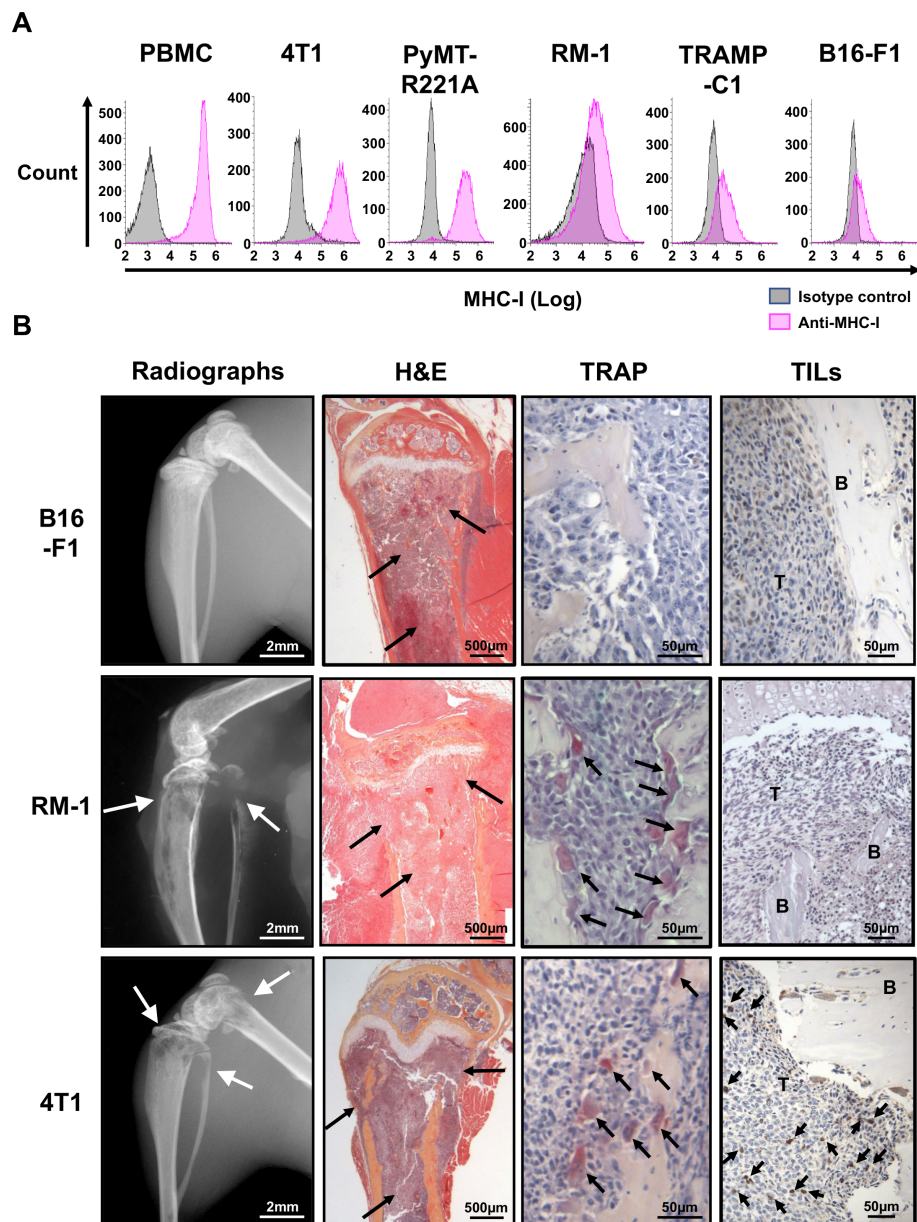
Fig. 1. T cells infiltrate the osteolytic bone metastases of MHC-I$^+$ 4T1 breast cancer cells in mice. (*A*) Flow cytometry analysis of MHC-I expression in mouse PBMCs, breast (4T1, PyMT-R221A), and prostate (RM-1, TRAMP-C1) cancer cells, and melanoma cells (B16-F1). The gray histogram corresponds to cells stained with an isotype control antibody and the pink one to cells stained with the antibody against MHC-I. (*B*) Bone metastasis caused by B16-F1 or 4T1 cancer cells inoculated in the left cardiac ventricle of C57BL/6 or Balb/C mice, and of RM-1 cells inoculated in the tibia of C57BL/6 mice. Results are shown as representative radiographs (arrows indicate osteolytic lesions), H&E-stained sections (arrows indicate bone metastases), sections with TRAP staining (arrows indicate osteoclasts), and immunostaining with an anti-CD3 antibody to detect TILs (T = tumor; B = bone matrix; arrows indicate T cells). H&E = hematoxylin and eosin; PBMC = peripheral blood mononuclear cell; TIL = tumor infiltrated lymphocyte.

pathological conditions, we measured the number of osteoclasts at the tumor-bone interface. TRAP staining indicated that there was a 1.95-fold increase of the amount of osteoclasts in bone metastases of Balb/C mice compared to Balb/C SCID (Fig. 2*C*). These results indicate that a functional immune system increased osteoclastogenesis and the development of bone metastases.

Because Balb/C SCID mice lack both T and B cells, to determine whether T cells mediated this effect, we specifically depleted T cells in wild-type mice. Balb/C mice were inoculated with 4T1 breast cancer cells and C57BL/6 mice with RM-1 prostate cancer cells to cause bone metastases and then received injections of a control antibody or antibodies against CD4 and CD8. T-cell depletion was then confirmed by flow cytometry (Supplemental Fig. S3*A*). Radiographic analysis indicated that in mice with T cells, there was a 1.83-fold increase of the osteolysis area, compared to T-cell depleted mice (Fig. 3*A*). Histomorphometric analysis indicated that the tumor area was increased
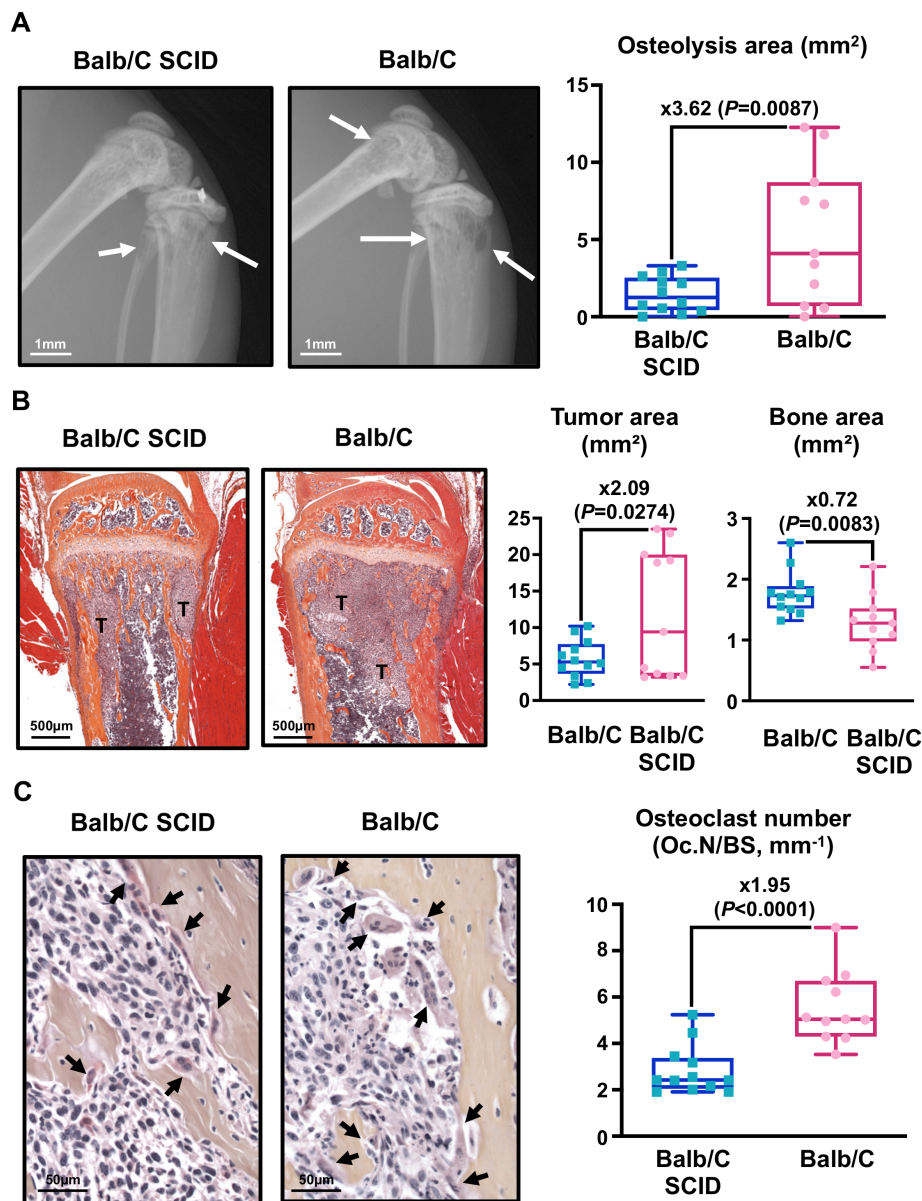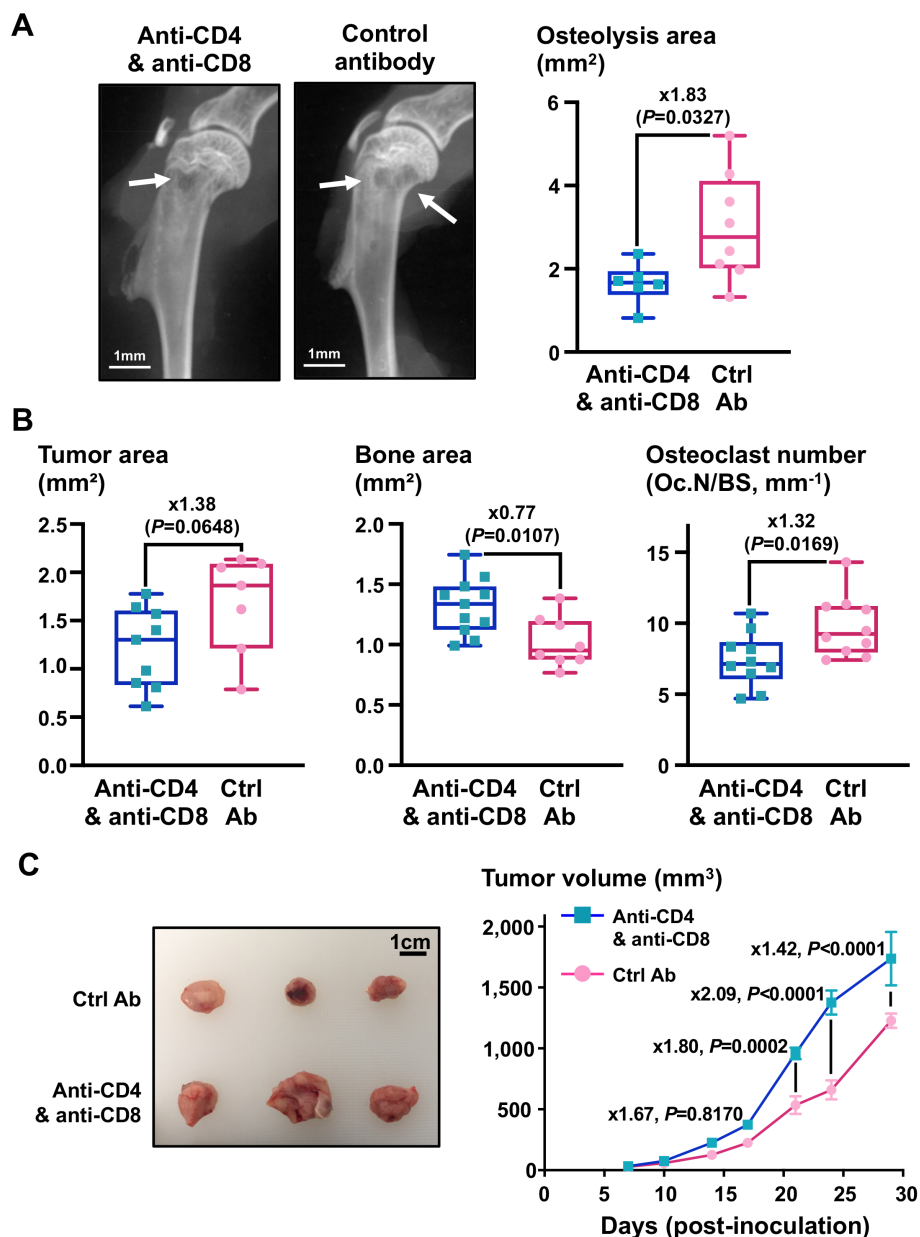
Fig. 2. Bone metastases from 4T1 cells are increased in mice with a functional immune system. 4T1 cells were inoculated in the left cardiac ventricle of Balb/C SCID ($n = 12$) or Balb/C mice ($n = 11$). (*A*) Representative radiographs from hindlimbs, 10 days after the inoculation (arrows indicate osteolytic lesions) and quantification of the osteolysis area on radiographs. (*B*) Representative H&E-stained sections of tibias (T, tumor) and histomorphometric analysis of tumor area (left graph) and bone area (right graph). (*C*) Representative images of bone sections after TRAP staining (arrows indicate osteoclasts) and quantification of the number of osteoclasts at the tumor bone interface. Results are shown as box plots, and were compared using an unpaired, two-tailed Student's *t* test. H&E = hematoxylin and eosin.

($\times 1.38$) in normal mice compared to T-cell depleted, although close to but not quite statistically significant ($p = 0.0648$) (Fig. 3*B*). However, similarly to the effect observed in the SCID mouse experiment, there was a significant decrease of the bone area ($\times 0.77$) and a significant increase of the number of osteoclasts at the tumor-bone interface in control mice compared to T-cell depleted mice ($\times 1.32$) (Fig. 3*B*). Interestingly, T-cell depletion did not have any effect on the osteolysis caused by RM-1 prostate cancer cells (Supplemental Fig. S3*B*), which is consistent with the lack of TILs in these bone metastases (Fig. 1*B*) and

indicate the effect of T-cell depletion in the 4T1 model would be caused by the depletion of anti-cancer T cells.

To confirm whether the pro-cancerous effect of T cells was specific to the bone tissue, we tested the effect of T-cell depletion on orthotopic tumors. When 4T1 breast cancer cells were inoculated in the mammary fat pad of Balb/C mice, treatment with anti-CD4 and anti-CD8 antibodies caused a significant increase of the tumor volume (Fig. 3*C*).

These results further emphasize that T cells specifically increase the development of osteolytic bone metastases, by

Fig. 3. Bone metastases from 4T1 are increased in mice with T cells, whereas orthotopic 4T1 tumor are decreased in mice with T cells. 4T1 cells were inoculated in the left cardiac ventricle or the 4th left mammary fat pad of Balb/C mice to cause bone metastases or orthotopic tumors. Mice received then a treatment with anti-CD4 and anti-CD8 antibodies (anti-CD4 and anti-CD8) or an isotype control antibody (Ctrl Ab). (A) Representative radiograph from forelimbs, 10 days after the inoculation (arrows indicate osteolytic lesions) and quantification of the osteolysis area on radiographs (anti-CD4 and anti-CD8, $n = 6$; control antibody, $n = 8$). (B) Histomorphometric analysis of tumor area, bone area, and osteoclast number at the tumor-bone interface of H&E stained sections of tibia of mice with 4T1 bone metastases with or without T-cell depletion. (C) Representative picture of 4T1 orthotopic tumors grown in mice with or without T-cell depletion and quantification of their volume ($n = 7$ per group). Results are shown as box plots (B,C) or as mean $\pm$ SEM, and were analyzed using an unpaired, two-tailed Student's t test (A,B) and a two-way ANOVA with Bonferroni's post-test (C). H&E = hematoxylin and eosin.

inducing an increased formation of osteoclasts at the tumor-bone interface.

Non-activated T cells increase osteoclast formation ex vivo whereas activated T cells inhibit osteoclast formation

To confirm the ability of T cells from 4T1 bone metastases to induce osteoclast formation, we performed an ex vivo osteoclastogenesis assay using mouse bone marrow cells cultured in the presence of M-CSF and RANKL. Surprisingly, the addition of T cells isolated from the bone marrow of mice inoculated with 4T1 breast cancer cells, using a cell sorter, suppressed the formation of osteoclasts ex vivo (Supplemental Fig. S4A), when T cells increased the number of osteoclasts in vivo (Figs. 2C, 3B). However, this effect was not directly due to the exogenous T cells added, but to the agonistic antibodies against

CD3 and CD28 added during the assay. Indeed, the mere addition of these antibodies prevented the formation of osteoclasts, even when we did not supplement the bone marrow culture with additional T cells (Supplemental Fig. S4A). These results suggest that the induced-activation of T cells from the bone metastases or from the bone marrow of the donor mouse could have an anti-osteoclastic effect. To prevent this artifact, we performed the next assays using the bone marrow of mice depleted of their T cells, using a treatment with an antibody against CD3. In addition, the isolated T cells were activated or not prior to their addition to the bone marrow culture. The direct addition of 10×10^3 T cells isolated from 4T1 bone metastases using a combination of

negative and positive selection with magnetic beads increased osteoclast formation (+59%), while T cells from the bone marrow of normal mice (not inoculated with 4T1) did not have any effect on osteoclast formation (Fig. 4A).

Using quantitative real-time PCR, we confirmed that T cells isolated from 4T1 bone metastases using a cell sorter have a higher expression of the pro-osteoclastic genes *Rankl* and *Tnfa* than T cells isolated from the spleen or of bone metastasis-free bone marrow (Fig. 4B). We also measured the expression of the anti-osteoclastic genePCRs *Ifng* and *Il4* produced by T cells in mice.[15] Although the expression of *Il4* was higher when compared to splenic and normal bone marrow T cells, we could not
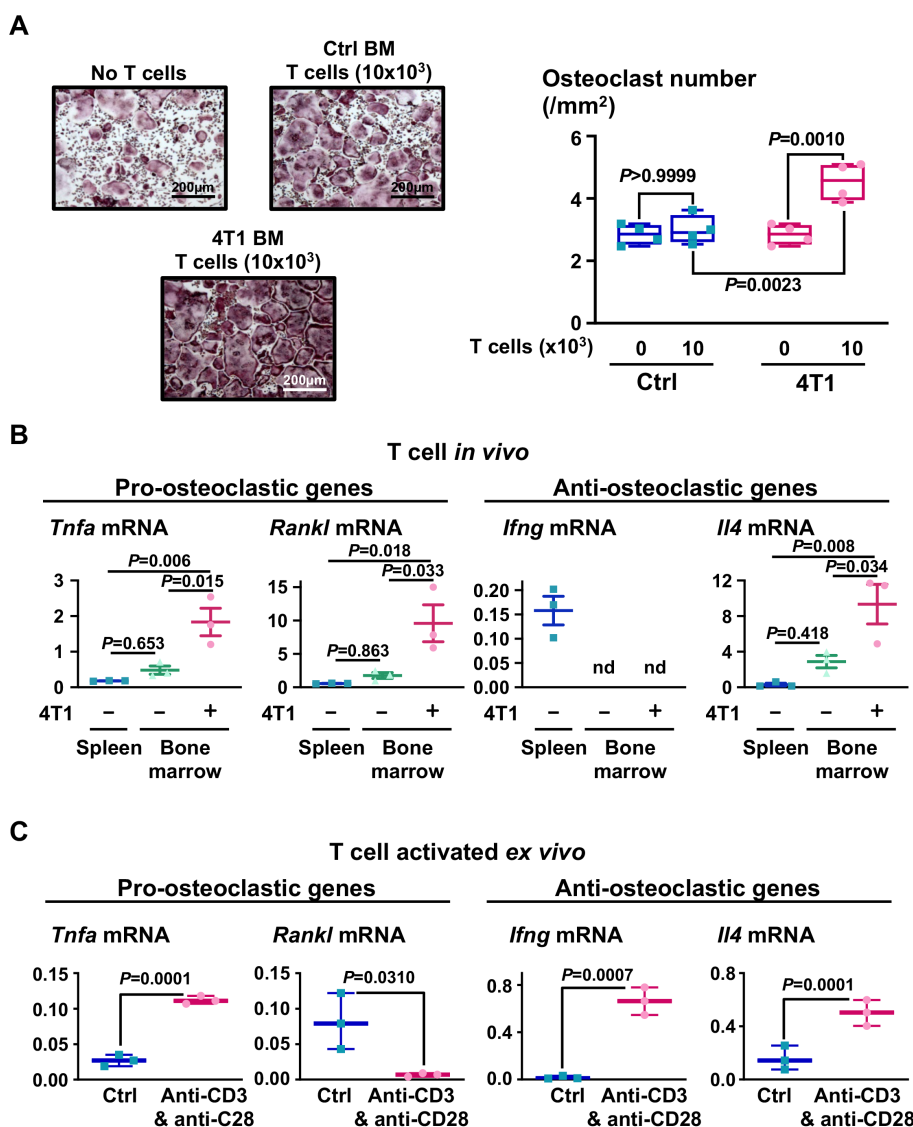
Fig. 4. T cells from bone metastases increase osteoclast formation ex vivo. (*A*) T cells were isolated from the BM of mice with or without 4T1 bone metastases and co-cultured with bone marrow cells in the presence of M-CSF (25 ng/mL) and RANKL (25 ng/mL) to induce osteoclastogenesis. Results are presented as (*left*) representative pictures the cells and (*right*) the number of osteoclasts (multinucleated TRAP$^+$ cells). Results are presented as box plots, and were compared using a two-way ANOVA with a Bonferroni post-test. (*B,C*) The expression of the pro-osteoclastic genes *Tnfa* and *Rankl* and the anti-osteoclastic genes *Ifng* and *Il4* was measured by quantitative real-time PCR in B. T cells isolated from the spleen or the bone marrow of mice with or without 4T1 bone metastases, or in (*C*) splenic T cells activated or not using anti-CD3 and anti-CD28 antibodies ex vivo. Results are presented as box plots, and were compared using a one-way ANOVA with a Tukey's post-test (*B*) or an unpaired, two-tailed Student's *t* test (*C*). BM = bone marrow.

detect the expression of *Ifng* in T cells from the bone marrow, with or without 4T1 bone metastases (Fig. 4B). The lack or low expression of these different genes in T cells from normal bone marrow is consistent with the absence of effect measured on osteoclast formation ex vivo (Fig. 4A) and on normal bone histology in vivo (Supplemental Fig. S2B). More importantly, the lack of expression of *Ifng* and expression of *Rankl* and *Tnfa* by T cells from 4T1 bone metastases is consistent with their capacity to increase osteoclast formation ex vivo (Fig. 4A) and in vivo (Fig. 3B), resulting in the increased development of 4T1 bone metastases in mice.

Different subsets of T cells, such as Th1 and Th2, have been demonstrated to directly inhibit osteoclastogenesis through IFNγ secretion and IL-4 secretion, respectively, while Th17 cells secreting IL-17 increase osteoblastogenesis.[15] By extension, we could expect that cytotoxic T cells producing IFNγ will inhibit osteoclasts, whereas Tc17 cells expressing IL-17 will increase osteoclast formation. Regulatory T cells (Tregs) do not appear to have a direct effect on osteoclasts on their own,[15] but could affect them indirectly by suppressing some other subset. To determine if the development of 4T1 bone metastases is associated with the expansion of a pro-osteoclastic subset of T cells or the decrease of an anti-osteoclastic subset, we compared the representation of these subset within the bone marrow of mice with or without bone metastases. We found that the amount of all the T cell subsets analyzed, Th1, Th2, Th17, Treg, cytotoxic T cells, and Tc17 cells, were decreased in 4T1 bone metastases compared to the bone marrow of healthy mice (Supplemental Fig. S4B). The decrease of T cells subsets that can produce IFNγ, Th1, and cytotoxic T cells is consistent with the lack of detection of *Ifng* messenger RNA (mRNA) in T cells from bone metastases and the pro-osteoclastic effect. However, there is no increase of any of the pro-osteoclastic subsets.

In absence of clear evidence of a subset that would explain the T cell-mediated increase of 4T1 bone metastases, we tested then the effect of the specific depletion of CD4+ or CD8+ T cells. Although a treatment of mice with an anti-CD4 antibody did not have any effect on the osteolytic lesions, an anti-CD8 antibody that causes the depletion of CD8+ T cells caused a significant 0.58-fold decrease of the osteolysis area compared to control mice (Supplemental Fig. S4C). This effect is similar to a co-treatment with anti-CD4 and anti-CD8 antibody that caused a 0.62-fold decrease. This result indicates then that it is not the CD4+ T cells that are driving an increase of 4T1 bone metastases but the CD8+ T cells that increase osteoclast formation and increase bone metastasis development in the 4T1 intracardiac model.

In addition to measuring gene expression in T cells isolated from mice, we also compared gene expression between T cells isolated from the spleen and activated or not activated ex vivo using the agonistic antibodies anti-CD3 and anti-CD28. There was a significant increase in the expression of *Ifng*, *Il4*, and *Tnfa*, as well as a decrease of *Rankl* in activated T cells compared to control ones (Fig. 4C). These differences in the expression of *Ifng*, *Il4*, and *Rankl* could explain the lack of osteoclast formation observed earlier (Fig. S3A). To test this effect, T cells were isolated from the spleen of normal mice using negative selection and magnetic beads. Splenic T cells were then activated or not activated ex vivo, using the lectin concanavalin A or agonistic antibodies for CD3 and CD28, during 7 days before adding them to bone marrow from a T-cell depleted mouse. The addition of 10×10^3 or 20×10^3 non-activated splenic T cells induced a significant increase of the number of osteoclasts, +13.7% and

+15.6%, respectively (Fig. 5A), similarly to T cells from 4T1 bone metastases. In sharp contrast, the addition of T cells activated ex vivo, inhibited the formation of osteoclasts (Fig. 5A). When we used concanavalin A to activate T cells, the addition of 5×10^3 or more T cells caused a dose-dependent decrease of the osteoclastogenesis (Fig. 5A). Splenic T cells activated ex vivo using coated anti-CD3 and soluble anti-CD28 antibodies appeared to be more potent, because the addition of only 2×10^3 activated T cells caused a 95% decrease of the formation of osteoclasts ($p < 0.0001$) (Fig. 5A). This anti-osteoclastic effect of activated T cells was not due to a bystander cytotoxic effect because an 3-(4,5-dimethylthiazol-2yl)-2,5-diphenyltetrazolium bromide (MTT) assay did not show differences in cell viability when adding activated or non-activated T cells to the culture (Supplemental Fig. S4C). The addition of antibodies neutralizing IFNγ and IL-4 in the co-culture did not have any effect individually. However, the combined inhibition of IFNγ and IL-4 partly reversed inhibition of osteoclastogenesis caused by activated splenic T cells (Supplemental Fig. S4D), suggesting that T-cell secreted IFNγ and IL-4 inhibit osteoclastogenesis, consistent with previous observations.[15]

Therefore, it seems that T cells can have very different effects on osteoclastogenesis: while non-activated T cells support the formation of osteoclasts, activated T cells inhibit it. Considering their gene expression and their pro-osteoclastic effect, these results suggest that T cells from bone metastases are not activated or could be suppressed by the bone metastasis microenvironment.

T cells in bone metastases are not activated and resistant to agonist factors

To assess whether T cells were activated in 4T1 bone metastases, we used flow cytometry to characterize the expression of CD69, the early activation marker CD69, and of CD62L, a late activation marker, not expressed in activated T cells. We only found a small amount of T cells in the bone marrow of cancer-free Balb/C mice ($0.64\% \pm 0.04\%$) and the presence of 4T1 bone metastases caused a significant decrease in the amount of T cells in the bone marrow ($0.26\% \pm 0.01\%$) (Fig. 5B). In 4T1 bone metastases, the amount of CD62L− T cells in the bone marrow increased within the T cell population ($23.5\% \pm 3.71\%$ versus $31.38\% \pm 8.28\%$ of T cells) compared to cancer-free mice although it did not reach statistical significance ($p = 0.0649$) (Fig. 5C). Similarly, there was an almost significant increase of CD69+ T cells ($13.95\% \pm 3.53\%$ versus $4.50\% \pm 0.92\%$, $p = 0.0540$) (Fig. 5D). Overall, these results indicate that only a fraction of the T cells (~15% or ~30%, depending on the marker) would be activated in 4T1 bone metastases and that the large majority of bone marrow T cells (>70–85%) are not activated, which would be consistent with their pro-osteoclastic effect, as well as the lack of detection of *Ifng* mRNA in gene expression analysis expression (Fig. 4B).

To determine whether T cells from bone metastases could be activated, bone marrow cells of mice with bone metastases were cultured ex vivo in activating conditions overnight and the expression of the early activation marker CD69 was evaluated. Neither concanavalin A or anti-CD3 and anti-CD28 agonistic antibodies were able to induce the activation of T cells from bone metastases, whereas T cells from the spleen could be activated in the same conditions (Fig. 5E). Thus, these results suggests that conditions of the bone metastasis microenvironment suppress the activation of T cells.
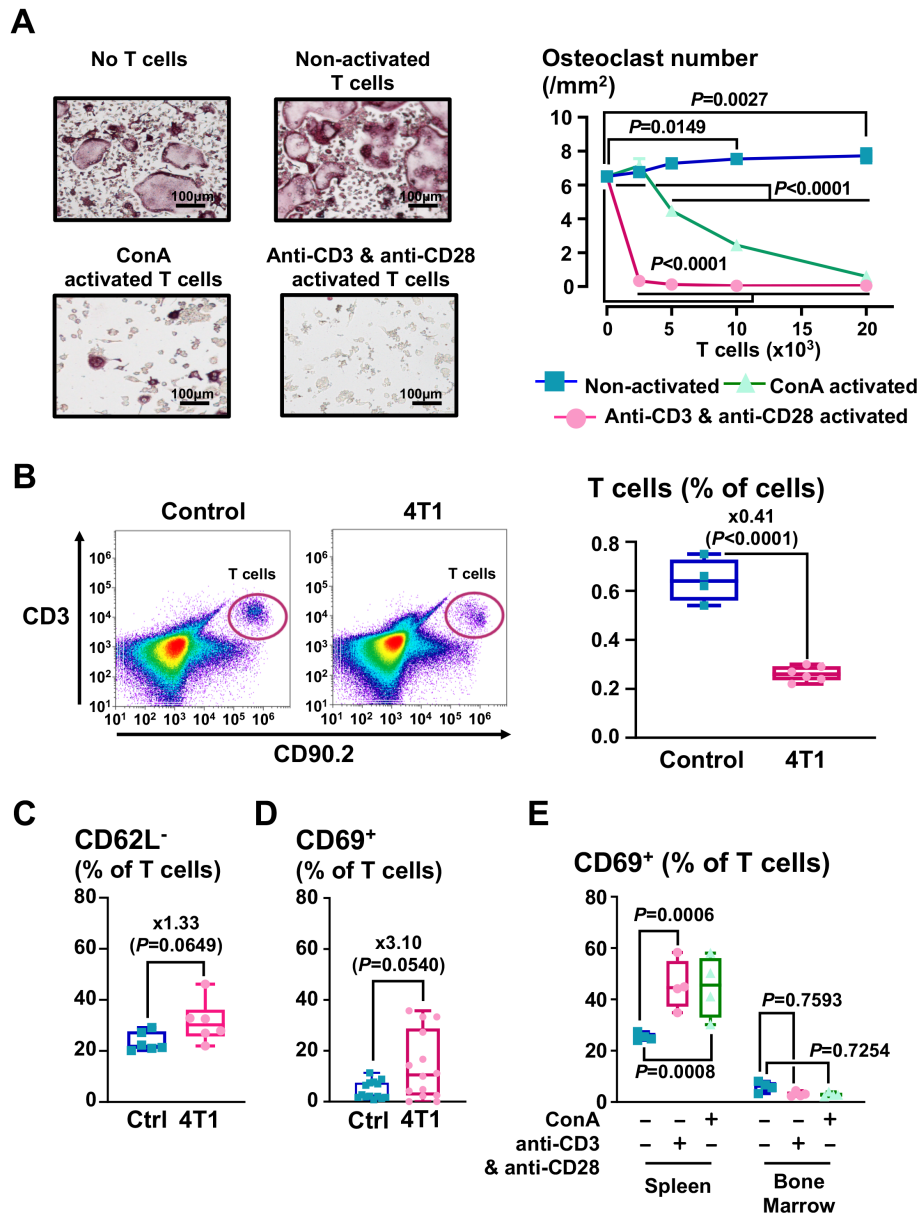
Fig. 5. Activated T cells prevent osteoclast formation ex vivo, while T cells from bone metastases are not and cannot be activated ex vivo. (*A,B*) T cells isolated from the spleen of normal mice were activated or not ex vivo using either ConA or anti-CD3 and anti-CD28 antibodies. Seven days later, T cells were added to a bone marrow culture in the presence of M-CSF (25 ng/mL) and RANKL (25 ng/mL). The number of osteoclasts (multinucleated TRAP$^+$ cells) was assessed 5 days later. (*A*) Representative pictures of the cells and quantification of the osteoclasts. Results are presented as the median and range number of osteoclasts and compared by using a two-way ANOVA with a Dunnett's post-test. (*B–E*) T cells from the bone marrow of Balb/C mice inoculated or not inoculated with 4T1 breast cancer cells in the left cardiac ventricle were analyzed using flow cytometry. Results are presented as (*B*) representative density plots of bone marrow cells to identify T cells (CD3$^+$ CD90.2$^+$ events), and the quantification of T cells (CD3$^+$ CD90.2$^+$ events) in the bone marrow and of the amount of CD62L$^-$ (*C*) and CD69$^+$ T cells (*D*) from in the bone marrow. (*E*) Splenocytes and bone marrow cells of mice with 4T1 bone metastases were treated or not treated overnight with the activator ConA or the agonistic antibodies anti-CD3 and anti-CD28 before analyzing the expression of CD69 on T cells, using flow cytometry. Quantitative results are presented as box plots and compared using a Mann-Whitney test (*C,D*) or a two-way ANOVA with Bonferroni post-test (*E*). ConA = concanavalin A.

Metabolically active and immunosuppressive MDSCs are increased in 4T1 bone metastases and monocytic-MDSCs express the PD-L1 immune checkpoint

We sought next to identify therapeutically relevant factors driving immunosuppression in bone metastases. During flow cytometry analysis of the bone marrow cells, we observed an increase in a cell population with a higher granularity (side scatter [SSC], Fig. 6A) characteristic of cells of the myeloid lineage. Such a cell population could be consistent with an increase of MDSCs, which were only reported as CD11b$^+$Gr1$^+$ cells, in bone metastases from breast and prostate cancer.[26,27] MDSCs are
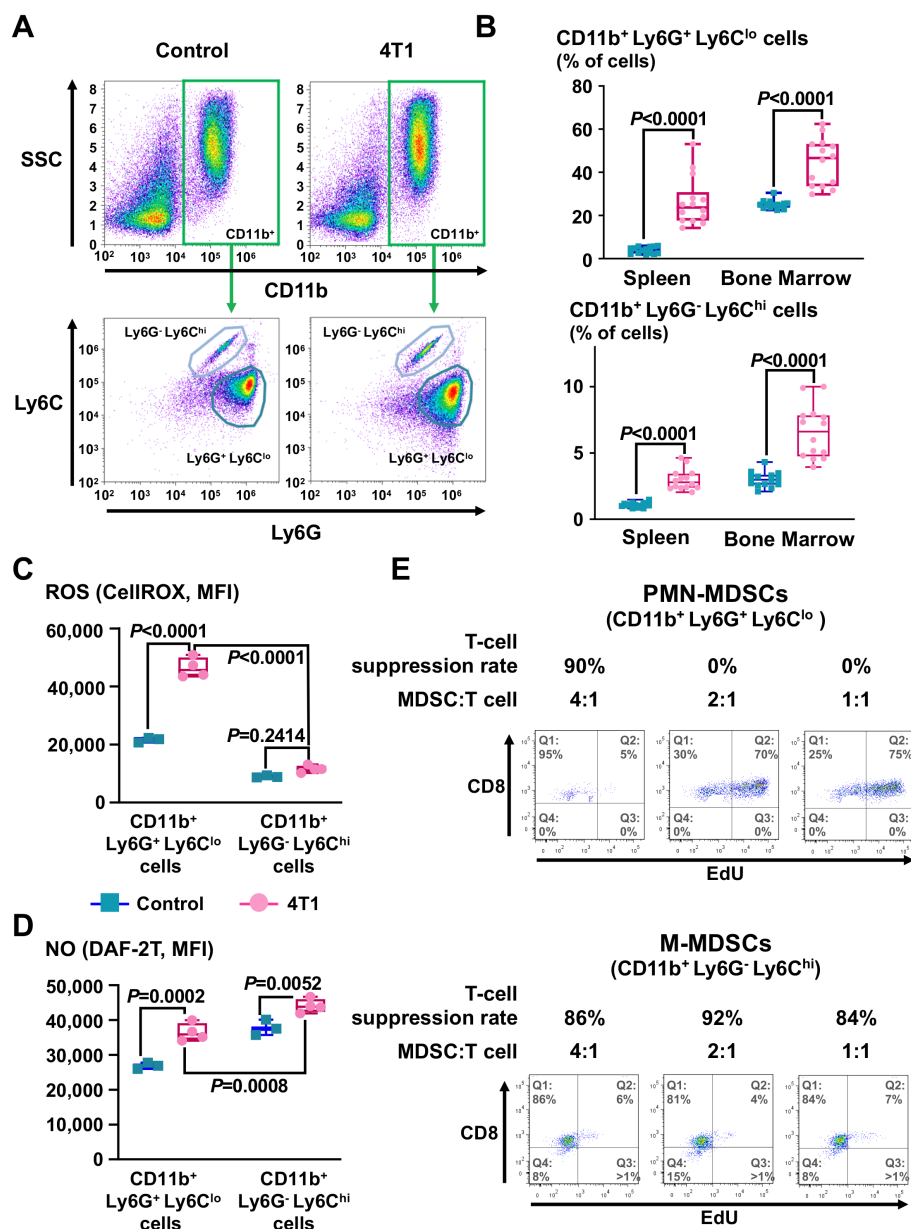
Fig. 6. Polymorphonuclear and monocytic MDSCs are increased in mice with 4T1 bone metastases. Mice were inoculated or not with 4T1 cells to cause bone metastases and cells were analyzed using flow cytometry 10 days later. (*A*) Representative pseudocolor dot plots of CD11b, Ly6G, and Ly6C expression on bone marrow cells. (*B*) Quantification of the amount of CD11b$^+$Ly6G$^+$Ly6C^{lo} and CD11b$^+$Ly6G$^-$Ly6C^{hi} cells in spleen and bone marrow cells (Control $n = 13$; 4T1 $n = 14$). (*C,D*) Quantification of the levels of (*C*) ROS and (*D*) NO as the MFI in CD11b$^+$Ly6G$^+$Ly6C^{lo} and CD11b$^+$Ly6G$^-$Ly6C^{hi} cells (Control $n = 3$; 4T1 $n = 4$). Quantitative results are presented as box plots and compared using a two-way ANOVA with Bonferroni's post-test. (*E*) Pseudocolor dot plots of Edu and CD8 levels in CD8$^+$ T cells co-cultured with CD11b$^+$Ly6G$^+$Ly6C^{lo} or CD11b$^+$Ly6G$^-$Ly6C^{hi} cells isolated from 4T1 bone metastases to assess their T-cell suppressive function. Representative dot plots of two independent experiments. MFI = mean fluorescence intensity; NO = nitric oxide; ROS = reactive oxygen species.

well known as suppressor of T-cell activation, and have been now further subdivided in polymorphonuclear MDSCs (PMN-MDSCs, CD11b$^+$Ly6G$^+$Ly6C^{lo}) and monocytic MDSCs (M-MDSCs, CD11b$^+$Ly6G$^-$Ly6C^{hi}).[28] Therefore, we characterized the amount of CD11b$^+$Ly6G$^+$Ly6C^{lo} and CD11b$^+$Ly6G$^-$Ly6C^{hi} cells in the spleen and bone marrow of mice with or without 4T1 bone metastases. The inoculation of 4T1 cells in the left cardiac ventricle of mice induced a significant increase in the spleen and the

bone marrow of the amount of cell populations with the phenotypic markers for PMN-MDSC and M-MDSC (Fig. 6*A,B*). As in most tumor models,[28] PMN-MDSC-like cells were more abundant than M-MDSC-like cells in the spleen (26.4% ± 3.0% versus 3.0% ± 0.2%), as well as in the bone marrow (44.7% ± 2.9% versus 6.6% ± 0.5%) (Fig. 6*B*). Beside the expression of these phenotypic markers, key functional characteristics are required to define PMN-MDSCs and M-MDSCs, including their capacity to

produce reactive oxygen species (ROS) or reactive nitrogen intermediaries (RNI) such as nitric oxide (NO), respectively. Staining of bone marrow cells with CellROX to detect ROS confirmed that $CD11b^+Ly6G^+Ly6C^{lo}$ cells are producing higher levels of ROS when mice where inoculated with 4T1 breast cancer cells and that the $CD11b^+Ly6G^+Ly6C^{lo}$ cells have higher levels of ROS when compared to $CD11b^+Ly6G^-Ly6C^{hi}$ cells in bone metastases (four-fold, $p < 0.0001$) (Fig. 6C). To detect NO, bone marrow cells were stained with DAF-2 diacetate. The presence of NO was detected in both subtypes of cells in the bone marrow and its levels were increased when mice were inoculated with 4T1 (Fig. 6D). As described previously,[28] $CD11b^+Ly6G^-Ly6C^{hi}$ cells have higher levels of NO when compared to the $CD11b^+Ly6G^+Ly6C^{lo}$ cells (1.2-fold, $p = 0.008$) (Fig. 6D).

We also tested the capacity of these cells to suppress T cell activation. $CD11b^+Ly6G^+Ly6C^{lo}$ and $CD11b^+Ly6G^-Ly6C^{hi}$ cells sorted from 4T1 bone metastases were co-cultured with splenic $CD8^+$ T cells from normal mice in activating conditions, for 72 hours before assessing T cell proliferation. $CD11b^+Ly6G^{+-}Ly6C^{lo}$ cells were able to suppress T cell proliferation but only at the highest effector:target ratio (4:1), whereas $CD11b^{+-}Ly6G^-Ly6C^{hi}$ cells were more potent suppressors, preventing T cell proliferation at the lowest effector:ratio test (1:1) (Fig. 6E).

Finally, we confirmed that, as reported,[29,30] these cells differentiate into osteoclasts. $CD11b^+Ly6G^+Ly6C^{lo}$ and $CD11b^{+-}Ly6G^-Ly6C^{hi}$ cells sorted from the bone marrow of normal mice and mice with 4T1 bone metastases were cultured in the presence of M-CSF and RANKL, ex vivo. $CD11b^+Ly6G^-Ly6C^{hi}$ cells that correspond to monocytes in normal mice were potent osteoclast progenitors when compared to $CD11b^+Ly6G^+Ly6C^{lo}$ cells that correspond more to granulocytes and neutrophils and need to be seeded at a higher density to form multinucleated $TRAP^+$ osteoclast-like cells (Supplemental Fig. S5). When $CD11b^+Ly6G^+Ly6C^{lo}$ and $CD11b^+Ly6G^-Ly6C^{hi}$ cells were obtained form 4T1 bone metastases, their capacity to differentiate toward osteoclasts decreased (Supplemental Fig. S5) suggesting that these cells have a decreased plasticity compared to cells of normal mice.

Taken together, these results clearly demonstrate that these $CD11b^+Ly6G^+Ly6C^{lo}$ and $CD11b^+Ly6G^-Ly6C^{hi}$ cells have the phenotypic, metabolic, and functional characteristics of MDSCs and that there is an expansion of PMN-MDSCs and M-MDSCs in 4T1 bone metastases that could contribute to osteoclastogenesis directly and indirectly by suppressing T cells in bone.

Molecules such as inhibitors of the phosphodiesterase-5 (PDE5), like sildenafil, or of bone resorption like the bisphosphonate zoledronic acid have been shown to inhibit the function or reduce the recruitment of MDSCs in colon and breast carcinoma models,[31,32] but not in bone metastases. Therefore, we tested the effect of treatments with sildenafil and zoledronic acid, alone or combined, in mice with 4T1 bone metastases. Although zoledronic acid was able to decrease the osteolytic lesions caused by 4T1 cells, sildenafil alone did not have any effect and the combination of both molecules did not cause a further decrease of osteolysis (Supplemental Fig. S6A). When we analyzed the MDSCs subtypes in 4T1 bone metastases, none of the treatments, alone or in combination, had any effect on the amount of PMN-MDSCs or M-MDSCs (Supplemental Fig. S6B), or the amount of ROS and NO they produced, respectively (Supplemental Fig. S6C). Consequently, there was only a slight change in the amount of T cells in bone metastases when mice were treated with both sildenafil and zoledronic acid compared to vehicle-treated mice (0.31% ± 0.06% versus 0.45% ± 0.10%,

$p = 0.0065$) and there was no change in the expression of the activation marker CD69 (0.95 ± 0.36 versus 0.84 ± 1.00, $p = 0.2486$) (Supplemental Fig. S6D). However, when we cultured the bone marrow cells of these mice ex vivo, the agonistic concanavalin A (ConA) and anti-CD3 and anti-CD28 antibodies were able to induce a significant increase of the amount of $CD69^+$ T cells (Supplemental Fig. S6E). It is then possible that the addition of an immunotherapeutic treatment to activate T cells in vivo could be combined to sildenafil and zoledronic acid.

Considering these results, we sought to determine the expression of actionable therapeutic markers related to immunotherapy on T cells in bone metastases. Treatments with immune checkpoints inhibitors, such as antibodies against CTLA-4, PD-1, and PD-L1, can lead to durable response in cancer patients with fewer associated side effects than chemotherapy. Therefore, we analyzed T cells from mouse bone marrow for the expression of immune checkpoints. The expression of CTLA-4 was detected in 26.0% ± 3.6% of T cells in the bone marrow of cancer-free mice and the inoculation of 4T1 breast cancer cells did not cause any changes (Fig. 7A). PD-1 was detected in 31.0% ± 4.9% of T cells from normal bone marrow, but its expression increased after the intracardiac inoculation of 4T1, and 70.3% ± 2.9% of T cells (×2.27) were $PD-1^+$ in 4T1 bone metastases (Fig. 7B). When we tested for the expression of its ligand, PD-L1, we found that there was a 46% increase of the number of $PD-L1^+$ cells in 4T1 bone metastases compared to normal bone marrow (5.5% ± 0.3% versus 3.8% ± 0.3%, respectively, $p = 0.0016$) (Fig. 7C). Expression of PD-L1 seems to be attributed to MDSCs because 9.7% of $PD-L1^+$ cells are PMN-MDSCs and 78.6% are M-MDSCs (Fig. 7D). Interestingly, although only 2.3% ± 0.3% of PMN-MDSCs are $PD-L1^+$, 79.7% ± 3.6% of M-MDSCs are $PD-L1^+$ in 4T1 bone metastases (Fig. 7E,F) and could then suppress the activation of $PD-1^+$ T cells causing their pro-osteoclastic effect.

Discussion

The immune system can target cancer cells for destruction, whether through components of the innate immunity, such as macrophages and NK cells, or T cells of the adaptive immune system that can specifically eliminate cancer cells.[33] However, one of the hallmarks of cancer cells is their ability to escape from or inhibit the immune response.[34] Immunotherapies have the potential to create an anti-cancer immune response (ie, tumor vaccines, chimeric antigen receptor T cells) or activate the host immune cells (ie, immune checkpoint inhibitors, bi-specific T-cell engager antibodies). Most of the immunotherapies focus on activating T cells against cancer cells and many have been successfully tested in the clinic, leading to increased survival and sustained long-term response in patients. However, it remains to be determined whether immunotherapies can cure patients with bone metastases or will put them at risk due to increased bone resorption mediated by T cells.

Although some laboratories started using humanized mice,[35] most bone metastasis models use immunodeficient mice inoculated with human cancer cells.[36] Therefore the effect of T cells in bone metastases is not well understood. Previous publications attempted to address this issue but found contrasting results when T cells either increased or decreased bone metastases.[12,14] To attempt to clarify this, we used different mouse cancer cell lines that can be used in syngeneic models when inoculated in immunocompetent mice of the same strain. Using 4T1 breast cancer cells, we found that there is infiltration of $CD3^+$
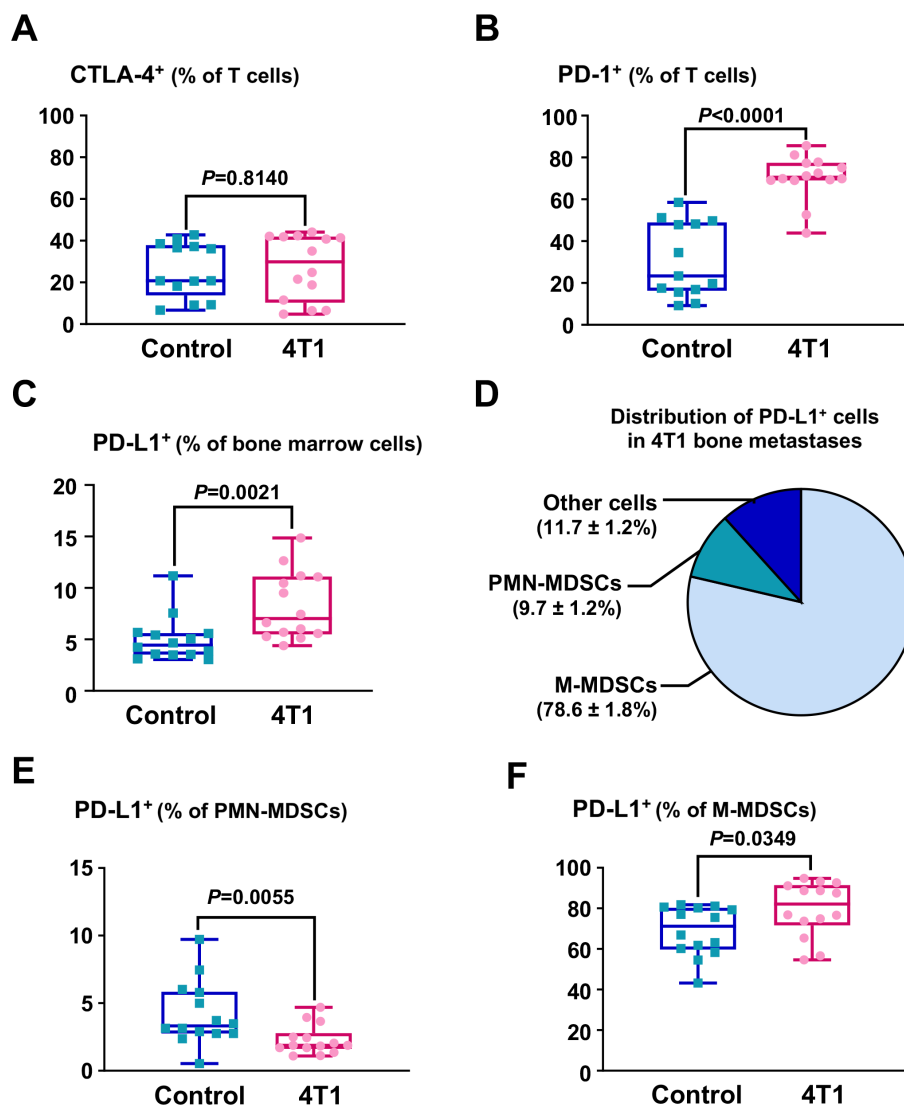
Fig. 7. Expression of immune checkpoints in T cells and MDSCs from bone marrow. Bone marrow cells from mice inoculated or not inoculated with 4T1 to cause bone metastases were analyzed using flow cytometry to quantify the amount of T cells expressing (*A*) CTLA-4 and (*B*) PD-1 of (*C*) bone marrow cells, (*E*) PMN-MDSCs, and (*F*) M-MDSCs expressing PD-L1 (Control $n = 13$; 4T1 $n = 14$). (*D*) Representation of the distribution of cells expressing PD-L1 in 4T1 bone metastases. Results are presented as box plots and compared using a Mann-Whitney *U* test (*B,E*) or an unpaired, two-tailed Student's *t* test (*A,C,F*).

T cells within the bone metastases and that T cells increase bone metastases, because mice lacking T cells, either SCID or T-cell depleted mice, had decreased levels of osteolysis. We could not clearly identify which specific subset of T cells is driving this osteoclastogenesis, however, it seems that the CD8$^+$ arm of the T cell family is responsible for it because depletion of CD8$^+$ T cells is enough to reverse this effect. Cytotoxic CD8$^+$ T cells and Tc17 cells were among the most abundant subset of T cells in 4T1 bone metastases, and IL-17 secretion of Tc17 cells could be responsible for the T-cell-induced osteoclastogenesis. This effect seems to be specific to the bone because T-cell depletion had the opposite effect in the mammary fat pad where it increased the tumor growth, suggesting that the effect of T cells in bone metastases could be due to the microenvironment.

The increase in the extent of 4T1 bone metastases could be due to either an increased homing of cancer cells to bone or an increased proliferation after the colonization of the bone marrow. Increased bone remodeling can increase the homing of cancer cells from blood to bone when released factors act as attractant.[37] We did not find differences between the bones of normal and SCID Balb/C mice using DXA and μCT analysis and previously published works indicated no significant differences in bone remodeling markers of immunodeficient nude mice or rat compared to immunocompetent ones.[16,38,39] Altogether, these results suggest that in the absence of infectious or pathological event there are no or little differences in the bone turnover of mice that could affect the homing of cancer cells to bone, and that T cells could affect cancer cell growth after settling in bone. This is reinforced by the similar results observed in T-cell depleted mice because there would not be difference in the bones of the mice at the time of the intracardiac inoculation, before the depletion. Considering that T cells can regulate

osteoclast formation and bone resorption, and that factors increasing bone resorption contribute to the vicious cycle of bone metastases, we focused on osteoclasts. In mice with T cells, we measured an increased amount of osteoclasts at the tumor-bone interface in 4T1 bone metastases. A similar effect of T cells on the formation of osteoclasts had been previously reported when T cells were under the influence of the primary breast cancer tumor[14] or in pathological conditions such as rheumatoid arthritis[15] or osteoporosis.[16] Circulating T cells from patients with osteolytic lesions due to myeloma, breast, prostate, or lung cancer also increased osteoclastogenesis ex vivo.[40,41] This effect was either due to T cell–derived TNF-α or RANKL and similar to these studies we found that T cells from bone metastases produce more TNF-α and RANKL than splenic T cells. Ex vivo, we confirmed that T cells isolated from 4T1 bone metastases increased the formation of osteoclasts in bone marrow culture assays, whereas T cells from normal bone marrow did not. This result suggest that it is tumor-infiltrating T cells and not other T cells from the bone marrow that affect osteoclasts. This observation is reinforced by results from the RM-1 prostate cancer model, where there is no T-cell infiltration within the bone metastases and no effect of T-cell depletion antibodies on the osteolytic area. Overall, these results suggest that it is tumor-infiltrating T cells that have a pro-osteoclastic effect and that increase the development of bone metastases.

Interestingly, the difference between the development of 4T1 bone metastases seemed to differ between the different immunodeficient mice. When compared to normal Balb/C mice, bone metastases were lower in SCID mice that lack T and B cell (−72%) than in T-cell depleted mice (−45%), suggesting that B cells could contribute to the difference. Previously published studies have found that B cells and B-lymphoid lineage cells can increase osteoclast differentiation.[42,43] This suggests that not only T cells but B cells could also participate to the development of 4T1 bone metastases by driving osteoclast and bone resorption.

Importantly, these data do not imply that immunotherapy should not be used for patients with bone metastases. Our data indicate that it is non-activated T cells that increase osteoclast formation whereas activated T cells have a drastically opposite effect and prevent osteoclast differentiation ex vivo. Consistent with this observation, we found that >70% to 80% of T cells in the bone metastases of 4T1 cells do not present an activated phenotype such as CD69+ or CD62L−, and we could not detect the Ifng mRNA expressed in some activated T cell subsets, including the cytotoxic CD8+ T cells. Immunotherapy could then be beneficial to patients by activating the anti-cancer properties of T cells in the skeletal tumor burden but also their anti-osteoclastic activity.

A preclinical study using an antibody against the checkpoint inhibitor CTLA-4 decreased the skeletal tumor burden caused by B16-FL melanoma cells, showing that activating T cells could decrease bone metastases.[12] In contrast, in this study, bone metastases from B16-F1 melanoma cells did not cause osteolysis and we could not detect T-cell infiltration. However, this difference of results could be due to the expression of the firefly luciferase in B16-FL cells, because luciferase can serve as a tumor-specific antigen that increases the immunogenicity of these cells.[44] Thus, in this model, there could be a T cell-based immune response, and T-cell infiltrated in the skeletal tumor burden could be activated by the anti-CTLA-4 antibody, reducing bone metastases. In a phase I clinical trial, treatment with paso-tuxizumab, a bispecific antibody that binds to the prostate-specific membrane antigen (PSMA) and CD3 of the T-cell receptor (TCR) to induce the recruitment of T cells caused a marked regression of bone metastases in one of 47 patients with castration-resistant prostate cancer.[45] Although the results of immunotherapy in clinic are promising, they appear to be limited to a small subset of patients as shown by the effect of paso-tuxizumab on the bone metastasis of one prostate cancer patient only,[45] or a response rate of 5% to 30% for patients with triple negative breast cancer with immune checkpoint inhibitors as monotherapy.[8]

The efficacy of immunotherapy can be limited by the intrinsic characteristics of cancer cells, including a low mutational tumor burden as reported in breast and prostate cancer[46] that decreases tumor foreignness and can limit T cell response. Poorly efficient immunotherapy can also be due to the local conditions within the tumor microenvironment,[47] which could occur in bone.

Bone is an important component of the life of T cells, as their precursors originate from the bone marrow, and some memory T cells are stored in the bone marrow where bone marrow stromal cells in mesenchymal niches suppress their activation.[48,49] Normal bone marrow is therefore unlikely to be a favorable microenvironment for anti-cancer T cells, and this may worsen in the context of bone metastases. Bone metastases are hypoxic[50] and have higher levels of TGF-β,[17] two factors that suppress the anti-cancer effect of T cells.[51,52] Other factors such as Treg, the third most abundant T cell subset we identified in 4T1 bone metastases, could be responsible for T cell inactivation in the bone marrow or the abundant MDSCs. In various studies, MDSCs were reported to accumulate in bone metastases, although they were only defined as CD11b+Gr1+, which corresponds to the early nomenclature and did not account for the main subtypes[26,27] or the studies focused on the PMN-MDSCs.[13,53] In this study, we further confirmed that PMN-MDSCs (CD11b+Ly6G+Ly6C^{lo}) accumulate in 4T1 bone metastases and that they are metabolically active, producing ROS, suppress T cell proliferation, and are the most abundant population of MDSCs. What we identify for the first time is that M-MDSCs (CD11b+Ly6G−Ly6C^{hi}) although less abundant than PMN-MDSCs, also expand in bone metastases and are more potent inhibitors of T cell proliferation than PMN-MDSCs, which could be due to their production of NO and the expression of PD-L1, especially because more than 70% of T cells in bone metastases express its receptor, the immune checkpoint PD-1. Interestingly, M-MDSCs from 4T1 bone metastases are potent osteoclast precursors, whereas the ability of PMN-MDSCs was much more limited, a property that had been suggested but not demonstrated so far.[53] Overall, these data confirm that the importance of MDSCs in bone metastases, as well as the importance to differentiate the distinct subsets, polymorphonuclear from neutrophilic and that M-MDSCs could be more functionally relevant to the development of bone metastases.

MDSCs are relevant therapeutic targets for the treatment of cancer and its complications, including bone metastases due to their capacity to differentiate to osteoclasts or suppress the anti-cancer immune response. Depletion of MDSCs using an antibody against Gr1 tended to decrease bone metastases from breast cancer cells and Lewis lung carcinoma cells in mice.[54] This effect was potentiated when the anti-Gr1 antibody was combined with the bone resorption inhibitor zoledronic acid.[54] If Gr1 is expressed on MDSCs and other myeloid cells in mice, it is not in human MDSCs.[28] Looking for alternative treatments that could be used in patients, we found that the PDE5 inhibitor sildenafil[31] and the bone resorption inhibitor zoledronic acid[32]

were reported to inhibit MDSCs in mouse models. However, neither treatment, alone or in combination, decreased the levels of PMN-MDSCs and M-MDSCs nor the levels of ROS and NO, responsible for the immunosuppression in these cells, nor increased the amount of T cells. More potent or directed treatments could be required to target MDSCs in bone metastases, as well as the combination with other immunotherapies. For example, RGX-104, an agonist of the liver-x nuclear receptor/Apolipoprotein E signaling, decreased the levels of MDSCs in mice and in cancer patients.[55] A combination of RGX-104 with the immune checkpoint inhibitor, anti-PD-1, was also more efficient at decreasing the development of B16-F10 melanoma and Lewis lung cancer cells in mice.[55] Because we found that almost 80% of T cells in 4T1 bone metastases are PD-1$^+$ and that almost 6% of bone marrow cells express its ligand PD-L1, predominantly the M-MDSCs, a similar combination RGX-104 and anti-PD-1 could be efficient at decreasing bone metastases. Combinations of immunotherapy like immune checkpoint inhibitors with chemotherapy also seems to be more effective. In triple-negative breast cancer patients, the combination of atezolizumab, an anti-PD-L1 antibody, with Nab-paclitaxel led to an increased progression-free and overall survival.[9]

In a castration-resistant prostate cancer model, Jiao and colleagues[56] found that the immune checkpoint inhibitors anti-PD-1 and anti-CTLA-4 reduced the development of subcutaneous tumors but not of bone metastases. In patients with non-small cell lung cancer, treatment with immune checkpoint inhibitors was also less efficient when patients had bone metastases as shown by a decreased overall survival.[10,57] These data suggest that the bone metastasis microenvironment can render immunotherapy ineffective, probably by suppressing T cell function, which is in line with our results as we found that T cells are not activated in bone and are difficult to activate ex vivo. However, it was possible to decrease the skeletal tumor burden in mice when combining the immune checkpoint inhibitors with an antibody neutralizing RANKL or TGF-β.[56] These results are important because they suggest that it is factors contained within the mineralized bone matrix and released during bone resorption, like TGF-β, that contribute to the immunosuppression and can limit the efficacy of immunotherapy. Neutralization of TGF-β was indeed associated with an increased activation of Th1 and cytotoxic T cells against prostate cancer cells in bone metastases.[56] In the 4T1 breast cancer model, we found that the PD-L1/PD-1 axis is also a relevant therapeutic target considering the amount of PD-L1$^+$ cells in the bone marrow, as well as the expression of PD-1 in more than 70% of T cells. Therefore, similar therapies combining immune checkpoint inhibitors with bone resorption inhibitors or anti-TGF-β treatment could be efficient against breast cancer bone metastases.

Conclusion

The efficacy of immunotherapy for the treatment of bone metastases and the effect of T cells in the development of bone metastases remain unclear. To address this problem, we used syngeneic mouse models of bone metastases and an ex vivo osteoclastogenesis assay. Our results show that non-activated T cells increase osteoclastogenesis and that CD8$^+$ T cells increase the development of bone metastases. This inactivation of T cells in bone metastases could be due to microenvironmental factors such as the expansion of metabolically active and functional MDSCs, including PD-L1$^+$ M-MDSCs that can differentiate into

osteoclasts and are potent suppressors of T cell activation. This could be explained by their production of immunosuppressive factors such as NO or the expression of PD-L1, the ligand of PD-1 present on more than 70% of T cells in bone. In contrast, T cells, when activated, suppressed the formation of osteoclasts. Therefore, the activation of T cells using immunotherapy could not only help T cells to kill cancer cells but could also prevent osteoclast formation and the bone loss associated to bone metastases in cancer patients.

AUTHOR CONTRIBUTIONS

Danna L. Arellano: Conceptualization; formal analysis; investigation; methodology; visualization; writing – original draft; writing – review and editing. **Patricia Juárez:** Funding acquisition; investigation; methodology; writing – review and editing. **Andrea Verdugo-Meza:** Formal analysis; investigation; methodology. **Paloma S. Almeida-Luna:** Formal analysis; investigation; methodology. **Juan A. Corral-Avila:** Conceptualization; formal analysis; investigation; methodology. **Florian Drescher:** Investigation. **Felipe Olvera:** Investigation. **Samanta Jiménez:** Investigation. **Bennett D. Elzey:** Conceptualization; formal analysis; investigation; methodology; supervision; visualization; writing – review and editing. **Theresa A. Guise:** Funding acquisition; supervision; writing – review and editing. **Pierrick GJ Fournier:** Conceptualization; formal analysis; funding acquisition; investigation; methodology; project administration; supervision; visualization; writing – original draft; writing – review and editing.

Conflict of Interest

The authors declare no conflict of interest regarding this work.

Data Availability Statement

The data that support the findings of this study are available from the corresponding author upon reasonable request.

References

1. Sung H, Ferlay J, Siegel RL, et al. Global Cancer Statistics 2020: GLOBOCAN estimates of incidence and mortality worldwide for 36 cancers in 185 countries. CA Cancer J Clin. 2021;71(3):209-249.

2. Coleman RE, Croucher PI, Padhani AR, et al. Bone metastases. Nat Rev Dis Prim. 2020;6(1):83.

3. O'Carrigan B, Wong MH, Willson ML, Stockler MR, Pavlakis N, Goodwin A. Bisphosphonates and other bone agents for breast cancer. Cochrane Database Syst Rev. 2017;10(10):CD003474.

4. Tesfamariam Y, Jakob T, Wockel A, et al. Adjuvant bisphosphonates or RANK-ligand inhibitors for patients with breast cancer and bone metastases: a systematic review and network meta-analysis. Crit Rev Oncol Hematol. 2019;137:1-8.

5. Farkona S, Diamandis EP, Blasutig IM. Cancer immunotherapy: the beginning of the end of cancer? BMC Med. 2016;14:73.

6. Loi S, Drubay D, Adams S, et al. Tumor-infiltrating lymphocytes and prognosis: a pooled individual patient analysis of early-stage triple-negative breast cancers. J Clin Oncol. 2019;37(7):559-569.

7. Vaddepally RK, Kharel P, Pandey R, Garje R, Chandra AB. Review of indications of FDA-approved immune checkpoint inhibitors per NCCN guidelines with the level of evidence. Cancers (Basel). 2020; 12(3):738.

8. Keenan TE, Tolaney SM. Role of immunotherapy in triple-negative breast cancer. J Natl Compr Canc Netw. 2020;18(4):479-489.

9. Schmid P, Adams S, Rugo HS, et al. Atezolizumab and Nab-paclitaxel in advanced triple-negative breast cancer. N Engl J Med. 2018; 379(22):2108-2121.

10. Landi L, D'Inca F, Gelibter A, et al. Bone metastases and immunotherapy in patients with advanced non-small-cell lung cancer. J Immunother Cancer. 2019;7(1):316.

11. Li X, Wang L, Chen S, et al. Adverse impact of bone metastases on clinical outcomes of patients with advanced non-small cell lung cancer treated with immune checkpoint inhibitors. Thorac Cancer. 2020; 11(10):2812-2819.

12. Zhang K, Kim S, Cremasco V, et al. CD8$^+$ T cells regulate bone tumor burden independent of osteoclast resorption. Cancer Res. 2011; 71(14):4799-4808.

13. Bidwell BN, Slaney CY, Withana NP, et al. Silencing of Irf7 pathways in breast cancer cells promotes bone metastasis through immune escape. Nat Med. 2012;18(8):1224-1231.

14. Monteiro AC, Leal AC, Goncalves-Silva T, et al. T cells induce pre-metastatic osteolytic disease and help bone metastases establishment in a mouse model of metastatic breast cancer. PLoS One. 2013;8(7):e68171.

15. Sato K, Suematsu A, Okamoto K, et al. Th17 functions as an osteoclastogenic helper T cell subset that links T cell activation and bone destruction. J Exp Med. 2006;203(12):2673-2682.

16. Cenci S, Weitzmann MN, Roggia C, et al. Estrogen deficiency induces bone loss by enhancing T-cell production of TNF-alpha. J Clin Invest. 2000;106(10):1229-1237.

17. Korpal M, Yan J, Lu X, Xu S, Lerit DA, Kang Y. Imaging transforming growth factor-β signaling dynamics and therapeutic response in breast cancer bone metastasis. Nat Med. 2009;15(8):960-966.

18. Hiraga T, Myoui A, Hashimoto N, et al. Bone-derived IGF mediates crosstalk between bone and breast cancer cells in bony metastases. Cancer Res. 2012;72(16):4238-4249.

19. Tauro M, Shay G, Sansil SS, et al. Bone-seeking matrix metalloproteinase-2 inhibitors prevent bone metastatic breast cancer growth. Mol Cancer Ther. 2017;16(3):494-505.

20. Baley PA, Yoshida K, Qian W, Sehgal I, Thompson TC. Progression to androgen insensitivity in a novel in vitro mouse model for prostate cancer. J Steroid Biochem Mol Biol. 1995;52(5):403-413.

21. Campbell JP, Merkel AR, Masood-Campbell SK, Elefteriou F, Sterling JA. Models of bone metastasis. J Vis Exp. 2012;67:e4260.

22. Wright LE, Buijs JT, Kim HS, et al. Single-limb irradiation induces local and systemic bone loss in a murine model. J Bone Miner Res. 2015; 30(7):1268-1279.

23. Schneider CA, Rasband WS, Eliceiri KW. NIH Image to ImageJ: 25 years of image analysis. Nat Methods. 2012;9(7):671-675.

24. Yin J, Selander K, Chirgwin J, et al. TGF-β signaling blockade inhibits PTHrP secretion by breast cancer cells and bone metastases development. J Clin Invest. 1999;103(2):197-206.

25. Untergasser A, Nijveen H, Rao X, Bisseling T, Geurts R, Leunissen JA. Primer3Plus, an enhanced web interface to Primer3. Nucl Acids Res. 2007;35(Issue suppl_2):W71-W74.

26. Danilin S, Merkel AR, Johnson JR, Johnson RW, Edwards JR, Sterling JA. Myeloid-derived suppressor cells expand during breast cancer progression and promote tumor-induced bone destruction. Oncoimmunology. 2012;1(9):1484-1494.

27. Park SI, Lee C, Sadler WD, et al. Parathyroid hormone-related protein drives a CD11b$^+$Gr1$^+$ cell-mediated positive feedback loop to support prostate cancer growth. Cancer Res. 2013;73(22):6574-6583.

28. Bronte V, Brandau S, Chen SH, et al. Recommendations for myeloid-derived suppressor cell nomenclature and characterization standards. Nat Commun. 2016;7:12150.

29. Sawant A, Deshane J, Jules J, et al. Myeloid-derived suppressor cells function as novel osteoclast progenitors enhancing bone loss in breast cancer. Cancer Res. 2013;73(2):672-682.

30. Zhuang J, Zhang J, Lwin ST, et al. Osteoclasts in multiple myeloma are derived from Gr-1$^+$CD11b$^+$ myeloid-derived suppressor cells. PLoS One. 2012;7(11):e48871.

31. Serafini P, Meckel K, Kelso M, et al. Phosphodiesterase-5 inhibition augments endogenous antitumor immunity by reducing myeloid-derived suppressor cell function. J Exp Med. 2006;203(12):2691-2702.

32. Melani C, Sangaletti S, Barazzetta FM, Werb Z, Colombo MP. Amino-biphosphonate-mediated MMP-9 inhibition breaks the tumor-bone marrow axis responsible for myeloid-derived suppressor cell expansion and macrophage infiltration in tumor stroma. Cancer Res. 2007;67(23):11438-11446.

33. Chen DS, Mellman I. Oncology meets immunology: the cancer-immunity cycle. Immunity. 2013;39(1):1-10.

34. Hanahan D, Weinberg RA. Hallmarks of cancer: the next generation. Cell. 2011;144(5):646-674.

35. Kahkonen TE, Suominen MI, Maki-Jouppila JHE, et al. Human immune system increases breast cancer-induced osteoblastic bone growth in a humanized mouse model without affecting Normal bone. J Immunol Res. 2019;2019:4260987.

36. Wright LE, Ottewell PD, Rucci N, et al. Murine models of breast cancer bone metastasis. Bonekey Rep. 2016;5:804.

37. Cox TR, Rumney RMH, Schoof EM, et al. The hypoxic cancer secretome induces pre-metastatic bone lesions through lysyl oxidase. Nature. 2015;522(7554):106-110.

38. Buchinsky FJ, Ma Y, Mann GN, et al. Bone mineral metabolism in T lymphocyte-deficient and -replete strains of rat. J Bone Miner Res. 1995;10(10):1556-1565.

39. Gao Y, Grassi F, Ryan MR, et al. IFN-gamma stimulates osteoclast formation and bone loss in vivo via antigen-driven T cell activation. J Clin Invest. 2007;117(1):122-132.

40. Colucci S, Brunetti G, Rizzi R, et al. T cells support osteoclastogenesis in an in vitro model derived from human multiple myeloma bone disease: the role of the OPG/TRAIL interaction. Blood. 2004;104(12): 3722-3730.

41. Roato I, Brunetti G, Gorassini E, et al. IL-7 up-regulates TNF-alpha-dependent osteoclastogenesis in patients affected by solid tumor. PLoS One. 2006;1:e124.

42. Manabe N, Kawaguchi H, Chikuda H, et al. Connection between B lymphocyte and osteoclast differentiation pathways. J Immunol. 2001;167(5):2625-2631.

43. D'Amelio P, Grimaldi A, Bernabei P, Pescarmona GP, Isaia G. Immune system and bone metabolism: does thymectomy influence postmenopausal bone loss in humans? Bone. 2006;39(3):658-665.

44. Baklaushev VP, Kilpelainen A, Petkov S, et al. Luciferase expression allows bioluminescence imaging but imposes limitations on the orthotopic mouse (4T1) model of breast cancer. Sci Rep. 2017;7(1):7715.

45. Hummel HD, Kufer P, Grullich C, et al. Pasotuxizumab, a BiTE® immune therapy for castration-resistant prostate cancer: phase I, dose-escalation study findings. Immunotherapy. 2021;13(2):125-141.

46. Alexandrov LB, Kim J, Haradhvala NJ, et al. The repertoire of mutational signatures in human cancer. Nature. 2020;578(7793):94-101.

47. Blank CU, Haanen JB, Ribas A, Schumacher TN. The "cancer immunogram". Science. 2016;352(6286):658-660.

48. di Nicola M, Carlo-Stella C, Magni M, et al. Human bone marrow stromal cells suppress T-lymphocyte proliferation induced by cellular or nonspecific mitogenic stimuli. Blood. 2002;99(10):3838-3843.

49. Glennie S, Soeiro I, Dyson PJ, Lam EW, Dazzi F. Bone marrow mesenchymal stem cells induce division arrest anergy of activated T cells. Blood. 2005;105(7):2821-2827.

50. Dunn L, Mohammad K, Fournier P, et al. Hypoxia and TGF-β drive breast cancer bone metastases through parallel signaling pathways in tumor cells and the bone microenvironment. PLoS One. 2009;4(9):e6896.

51. Kumar V, Gabrilovich DI. Hypoxia-inducible factors in regulation of immune responses in tumour microenvironment. Immunology. 2014;143(4):512-519.

52. Thomas DA, Massague J. TGF-β directly targets cytotoxic T cell functions during tumor evasion of immune surveillance. Cancer Cell. 2005;8(5):369-380.

53. Edgington-Mitchell LE, Rautela J, Duivenvoorden HM, et al. Cysteine cathepsin activity suppresses osteoclastogenesis of myeloid-derived suppressor cells in breast cancer. Oncotarget. 2015;6(29):27008-27022.

54. Capietto AH, Lee S, Clever D, et al. Effective treatment of established bone metastases can be achieved by combinatorial osteoclast blockade and depletion of granulocytic subsets. Cancer Immunol Res. 2021;9(1412):1400-1412.

55. Tavazoie MF, Pollack I, Tanqueco R, et al. LXR/ApoE activation restricts innate immune suppression in cancer. Cell. 2018;172(4):825-840.

56. Jiao S, Subudhi SK, Aparicio A, et al. Differences in tumor microenvironment dictate T helper lineage polarization and response to immune checkpoint therapy. Cell. 2019;179(5):1177-1190.

57. Qin A, Zhao S, Miah A, et al. Bone metastases, skeletal-related events, and survival in patients with metastatic non-small cell lung cancer treated with immune checkpoint inhibitors. J Natl Compr Canc Netw. 2021;19(8):915-921.